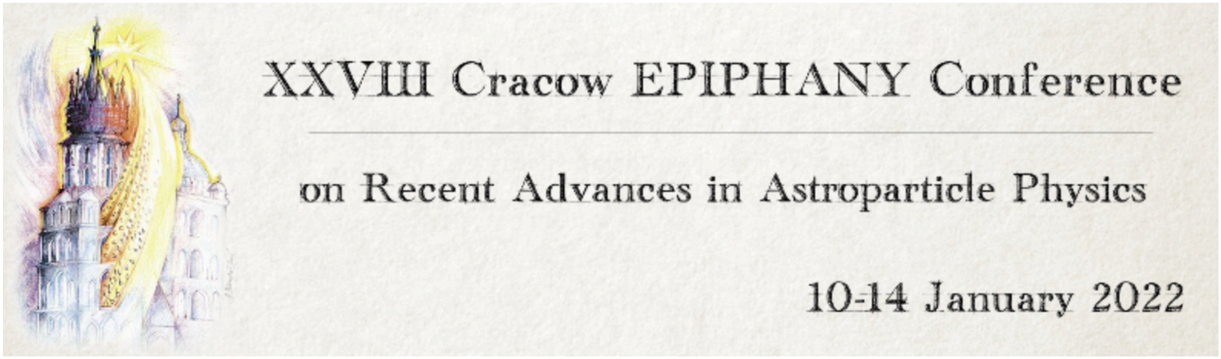

Galactic magnetars as transient ultra high energy cosmic ray sources

V. Voitsekhovskyi, R. Hnatyk
Astronomical Observatory of Taras Shevchenko National University of Kyiv

2022

Cosmic rays

- Maximum registered cosmic ray energy:
  $E_{max} = 3 \cdot 10^{20} eV$
- Ultra high energy cosmic rays (UHECR):
  $E \geq 10^{18} eV$
- Extreme high energy cosmic rays (EHECR):
  $E \geq 10^{20} eV$
- Exact sources of high energy cosmic rays remains unknown

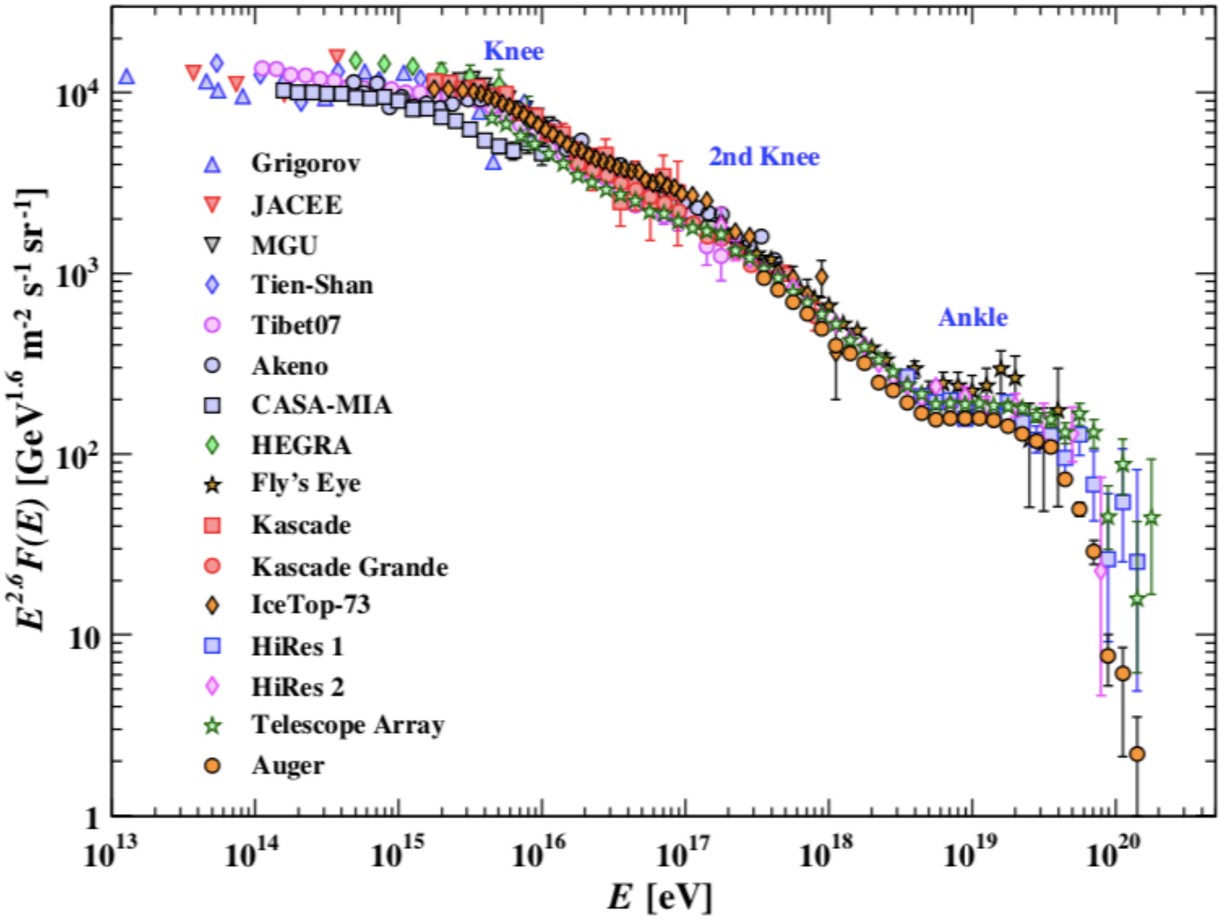

[Patrignani et al. 2016]

Cosmic rays: present and future detectors

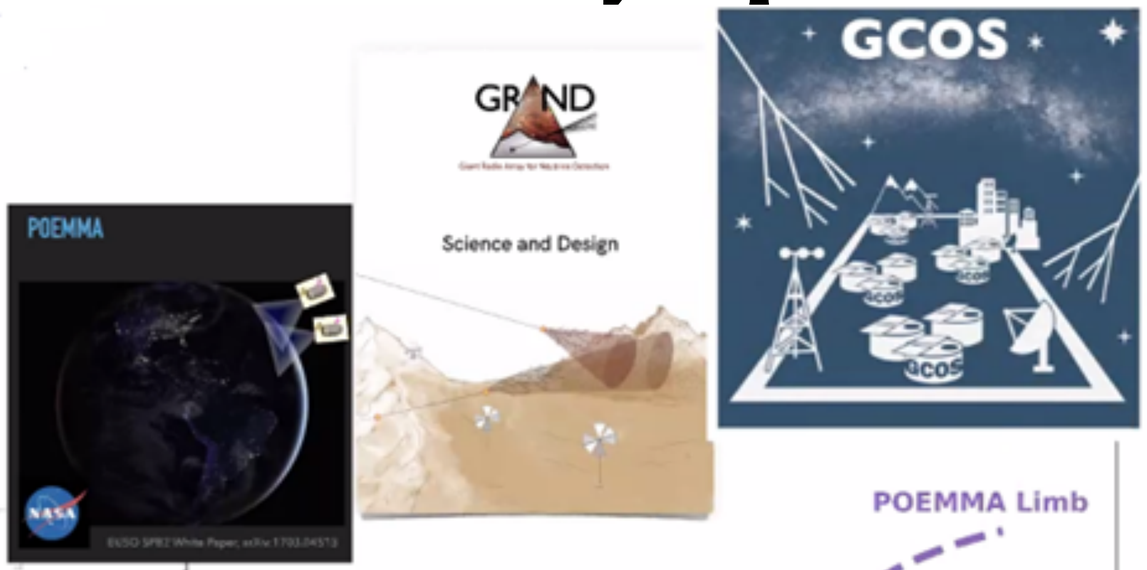

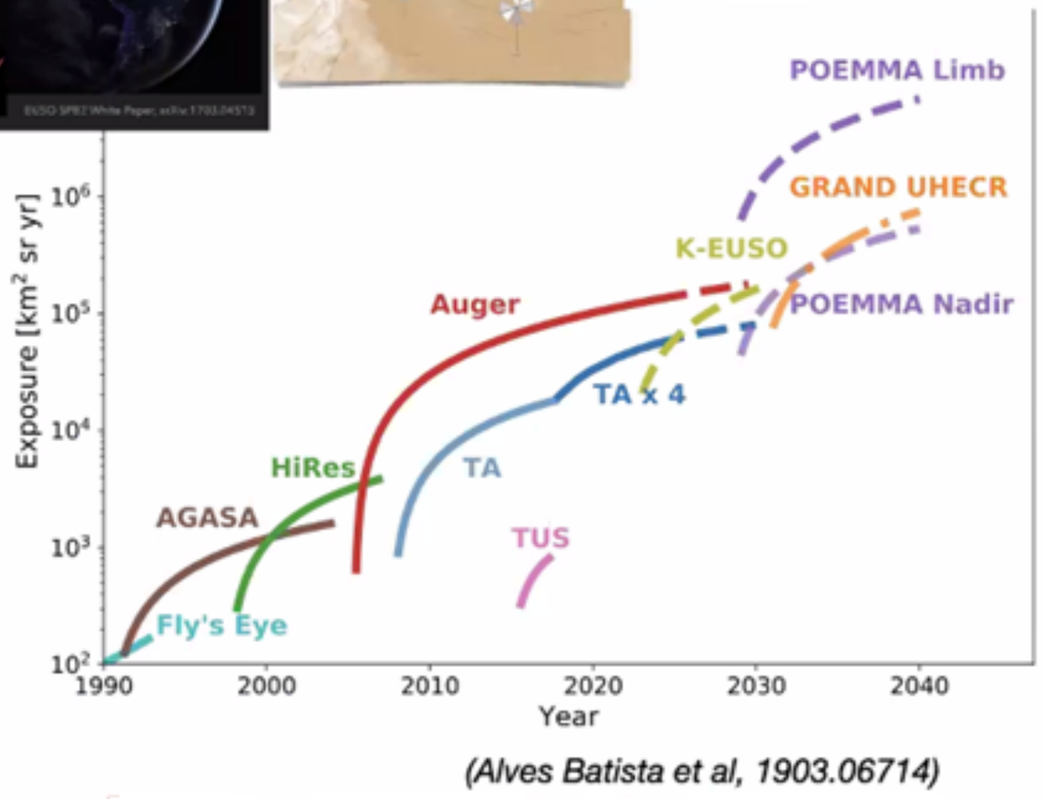

(Alves Batista et al, 1903.06714)

Telescope Array and Pierre Auger Observatory are the main state-of-the-art detectors

Energy spectrum and chemical composition of UHECR: recent Auger and TA data

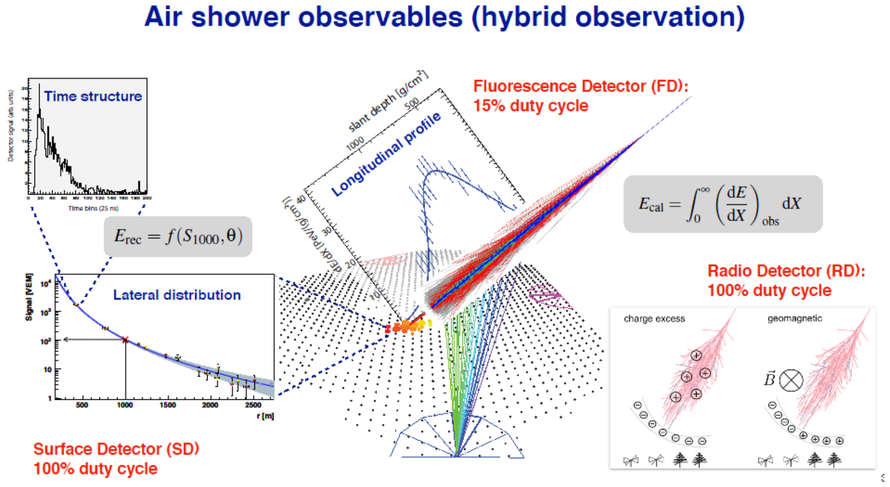

Modern technical principles of CR detection

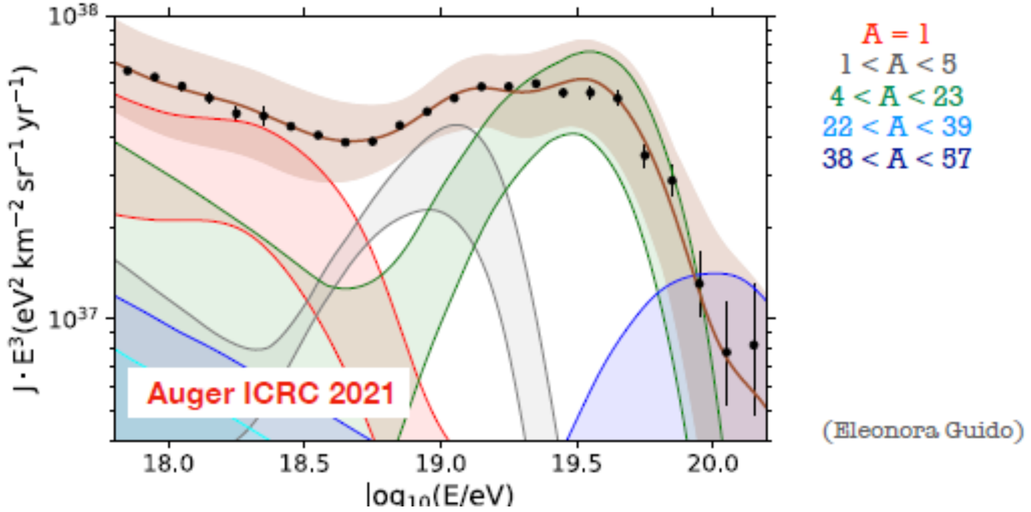

(Eleonora Guido)

Chemical composition

Spectrum with highlighted main features

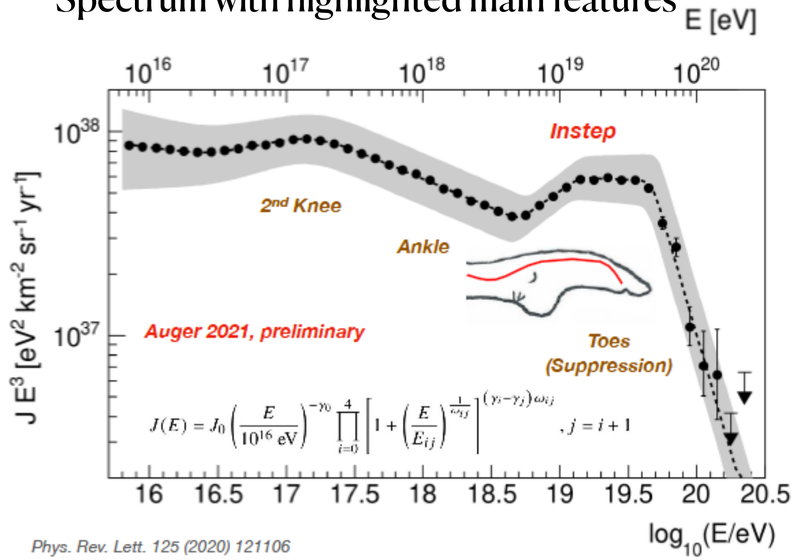

Phys. Rev. Lett. 125 (2020) 121106
Phys. Rev. D102 (2020) 062005

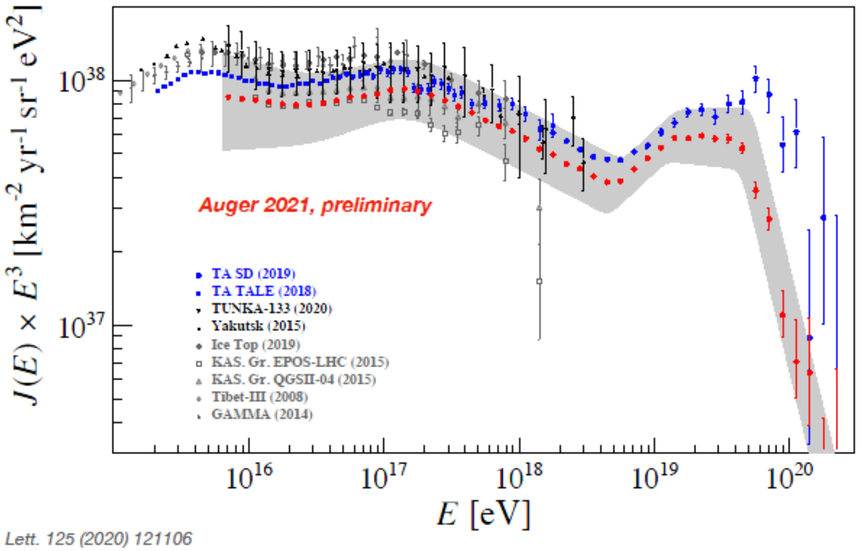

Phys. Rev. Lett. 125 (2020) 121106
Phys. Rev. D102 (2020) 062005
submitted to Eur. Phys. J. C (2021)

(Vladimir Novotny)

Figures from Ralph Engel PoS (ICRC2021)021

Cosmic rays: acceleration problems

Strong magnetic fields and/or big sizes of accelerators are need to achieve high energies of particles

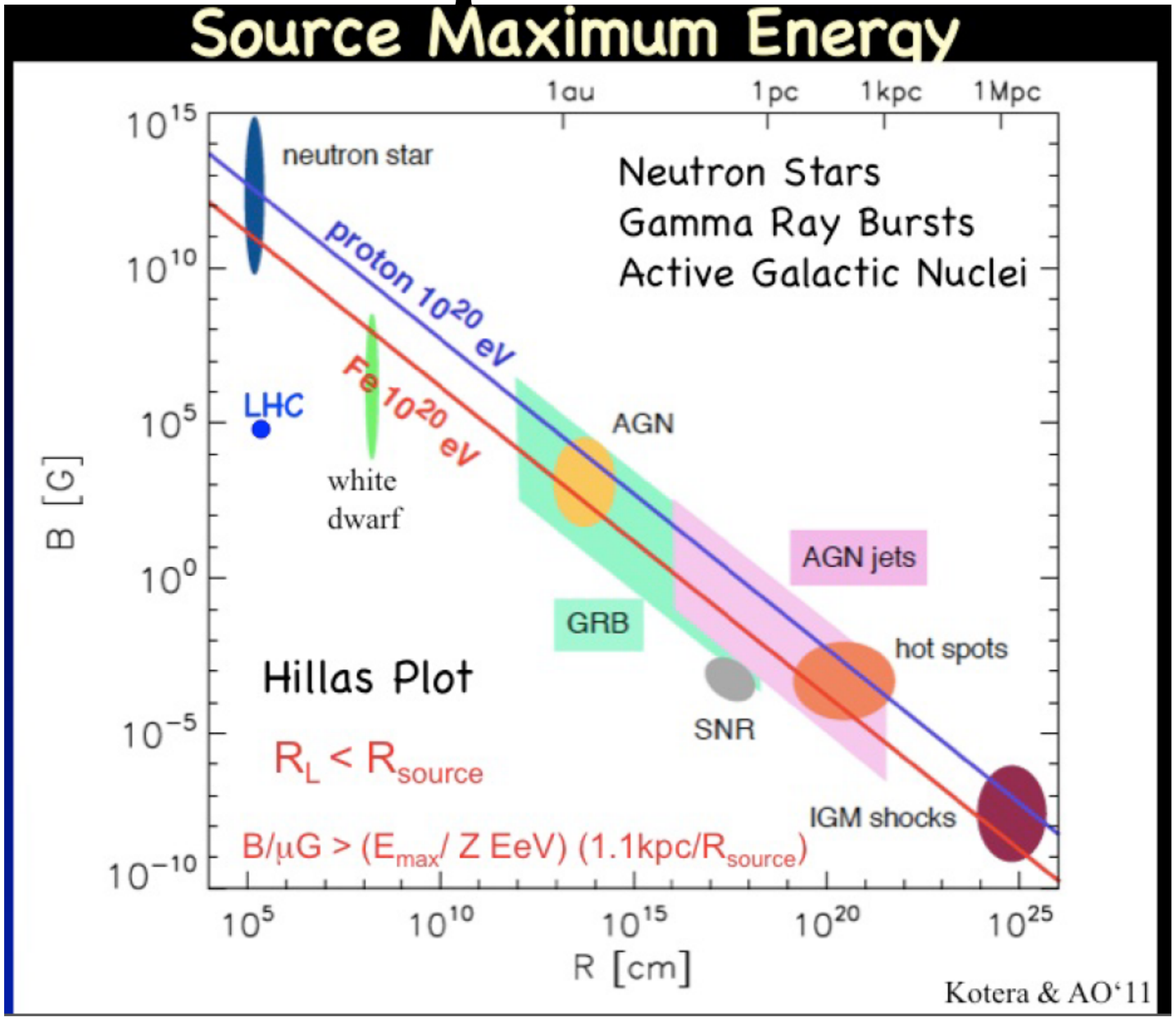

Acceleration sites for high energy cosmic rays

AGN:

acceleration on shock waves in jets

Galaxy clusters:

acceleration on shock waves in the intracluster medium

Compact objects:

pulsars, magnetars, gamma-ray bursts

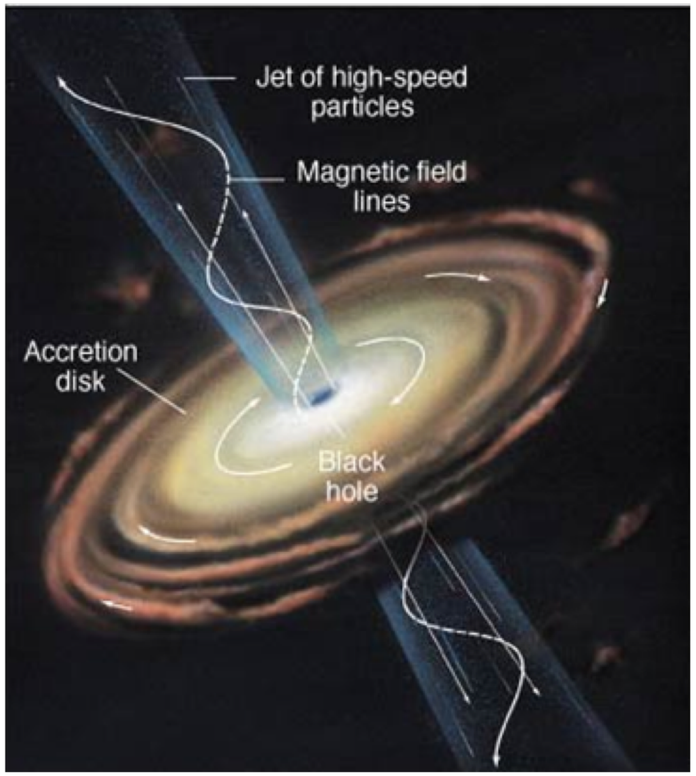

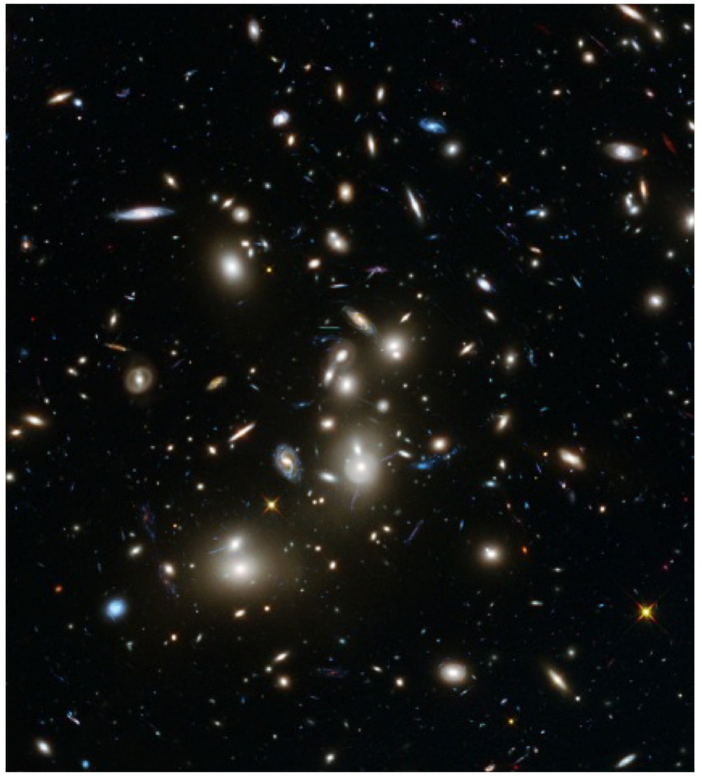

Restriction on UHECR sources: the energy-loss horizon λ of UHECR protons and nuclei as function of energy

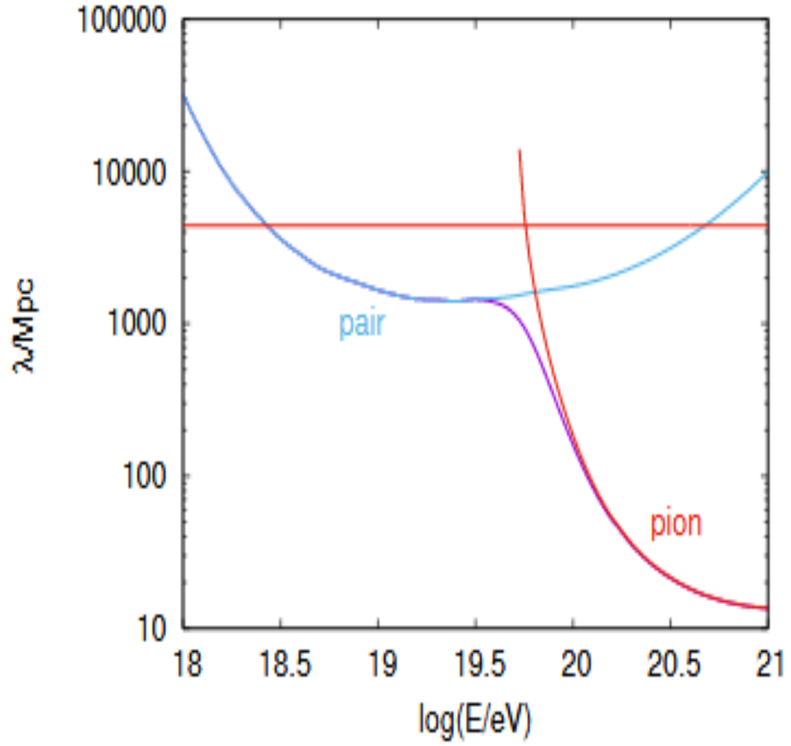

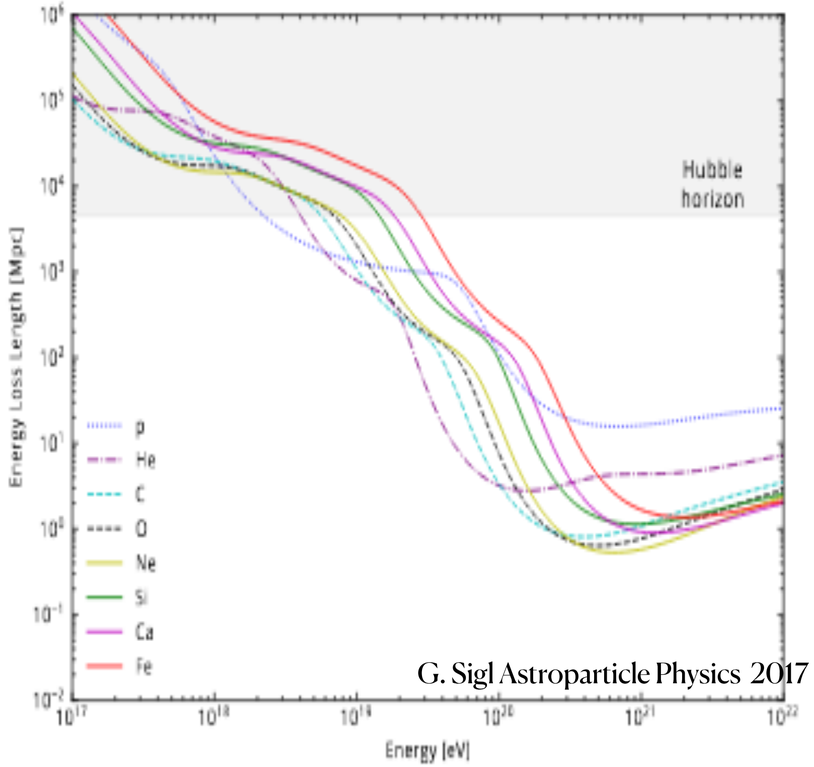

G. Sigl Astroparticle Physics 2017

For $E > 10^{20}$ eV EHECR:

- sources of protons and Fe-nuclei should be inside 30-50 Mpc
- sources of He and C-N-O nuclei should be inside 10-30 Mpc

Inside 50 Mpc EHECR can be accelerated in (mildly) relativistic transient jets in GRB, TDE and, most frequently, in giant flares of magnetars and in magnetar wind nebulae, created by newborn millisecond magnetars

$$\frac{E_{max}}{10^{20}eV} \lesssim \frac{Ze}{10^{20}eV}\left(\frac{L_{kin}\beta}{c\Gamma^2}\right)^{1/2} = 0.1Z\left(\frac{L_{kin}}{10^{45.5}erg/s}\right)^{1/2}\left(\frac{\Gamma^2/\beta}{100}\right)^{-1/2}$$

Map of EHECR events

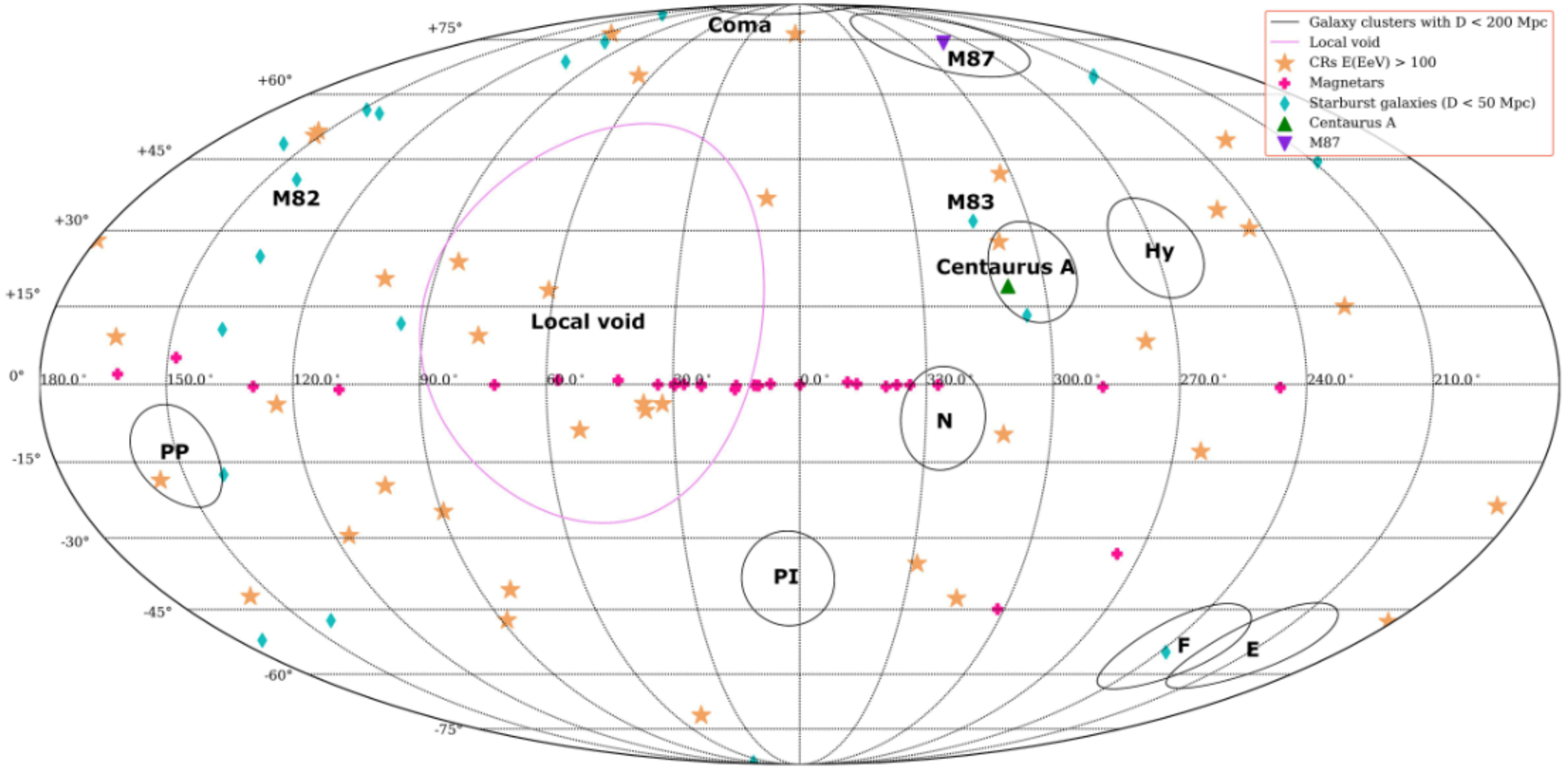

Figure 1: Sky positions of EHECR sample together with positions of some potential sources and clusters/superclusters of galaxies, that determine a large-scale mass distribution in the Local Universe.

Hnatyk & Voitsekhovskyi, PoS ICRC(2021) 464

Problem of source identification

To reduce such problems:

- considering events with high energies $E > 10^{20} eV$
- taking into account modern magnetic field models

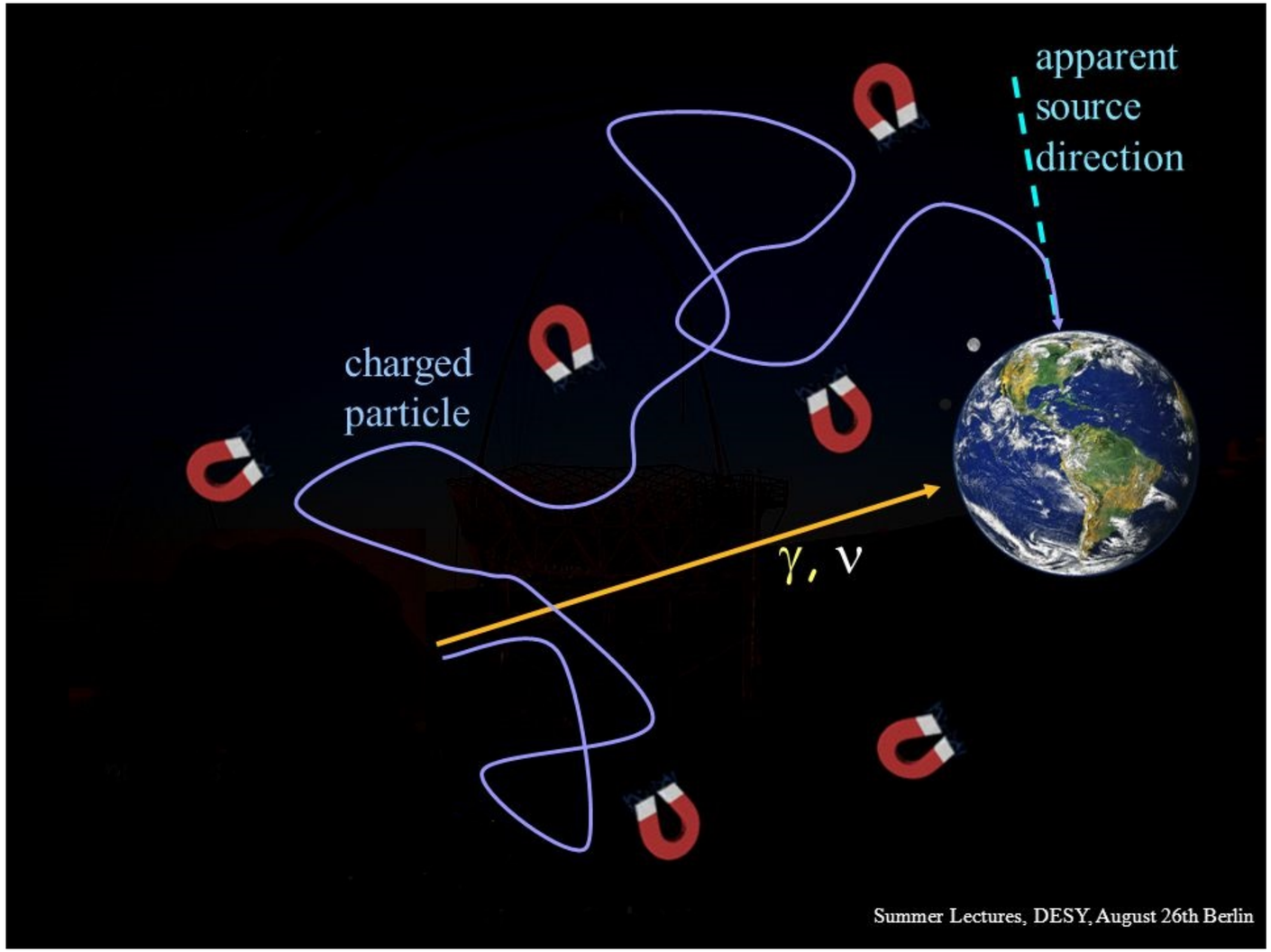

Backtracking trajectories of EHECR events

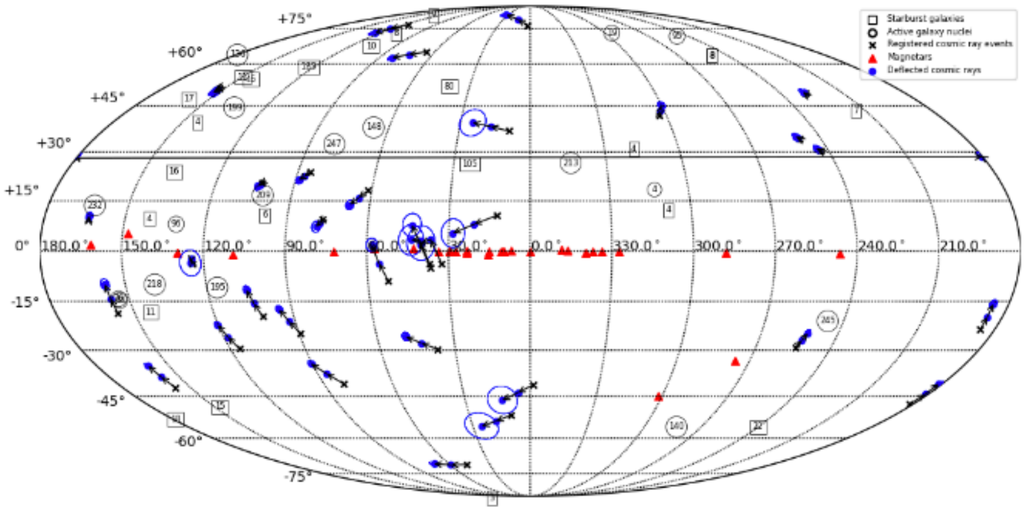

(a) Z=1, 2

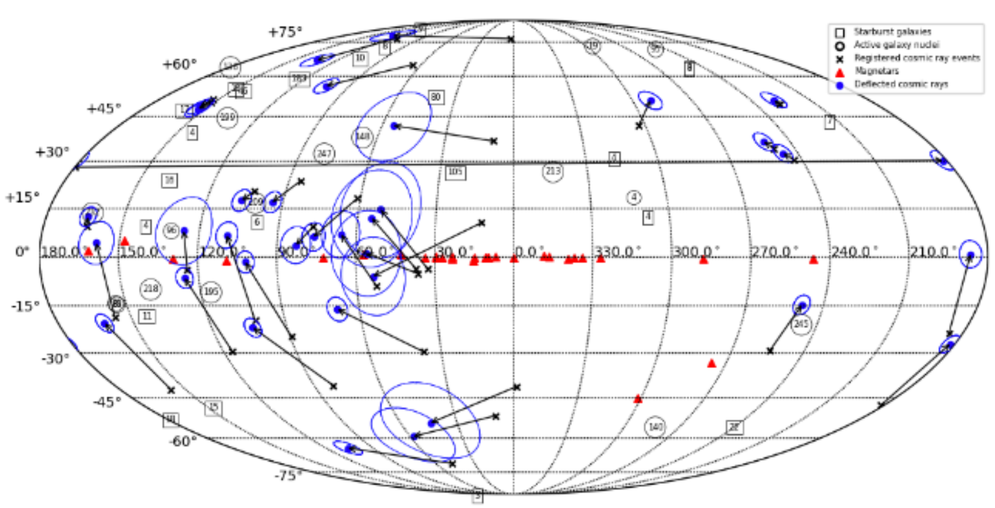

(b) Z = 6

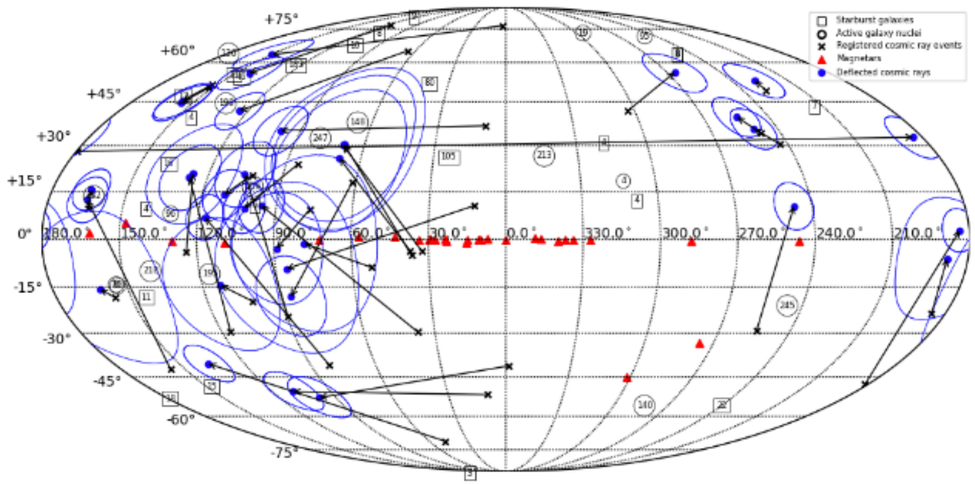

(c) Z=14

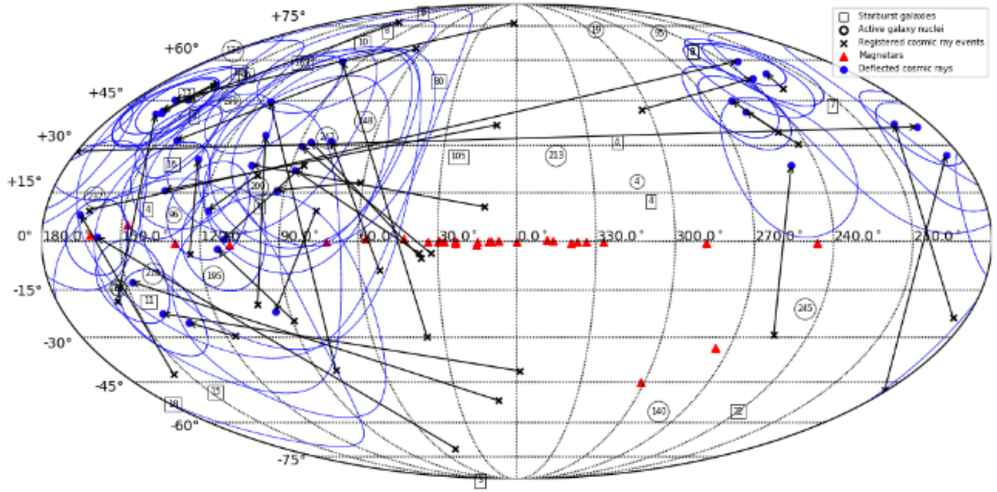

(d) Z = 26

Hnatyk & Voitsekhovskyi, PoS ICRC(2021) 464

Backtracking trajectories of the EHECR triplet of events

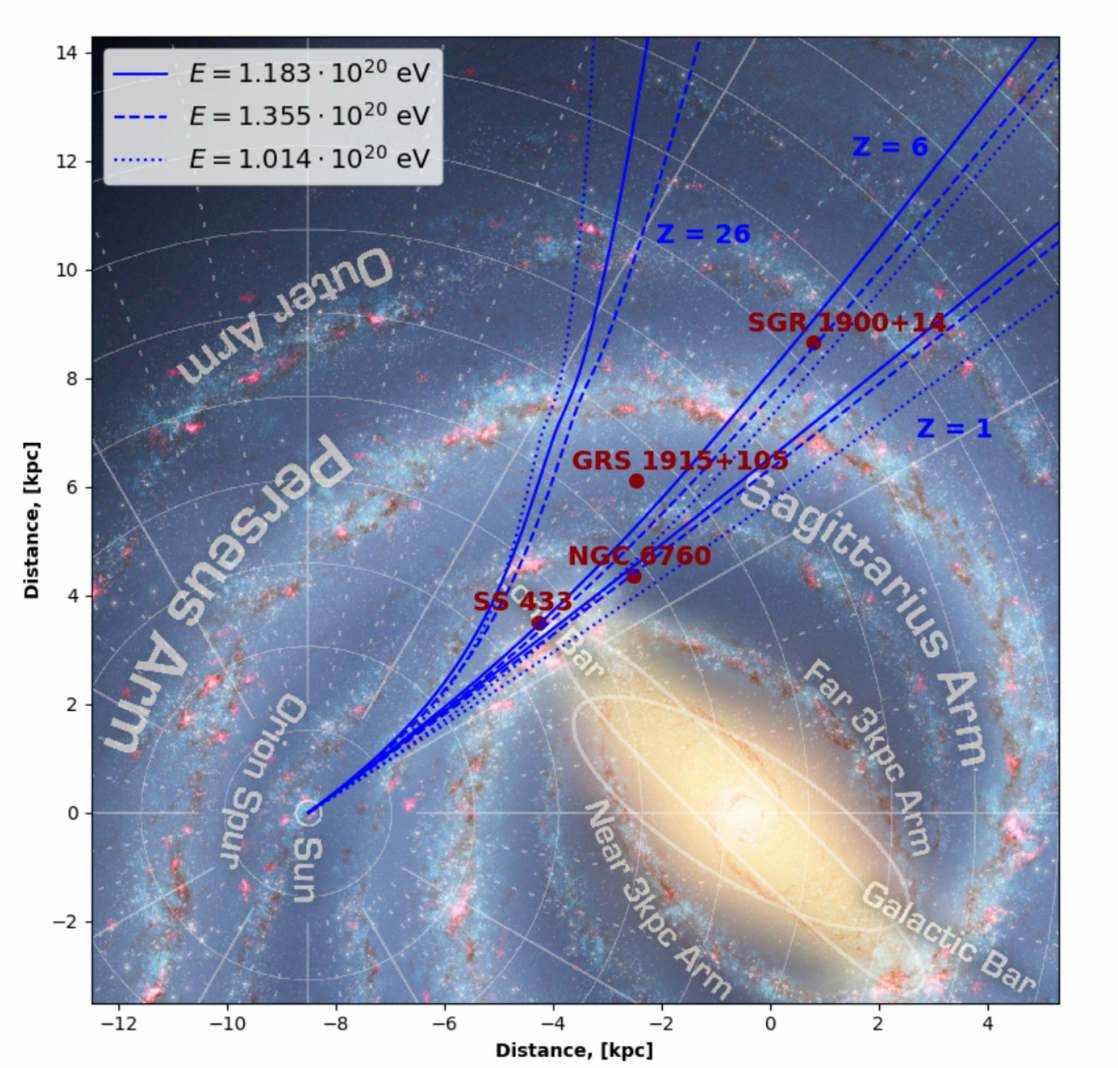

Calculated backward trajectories of EHECR triplet based on JF12 Galactic magnetic field

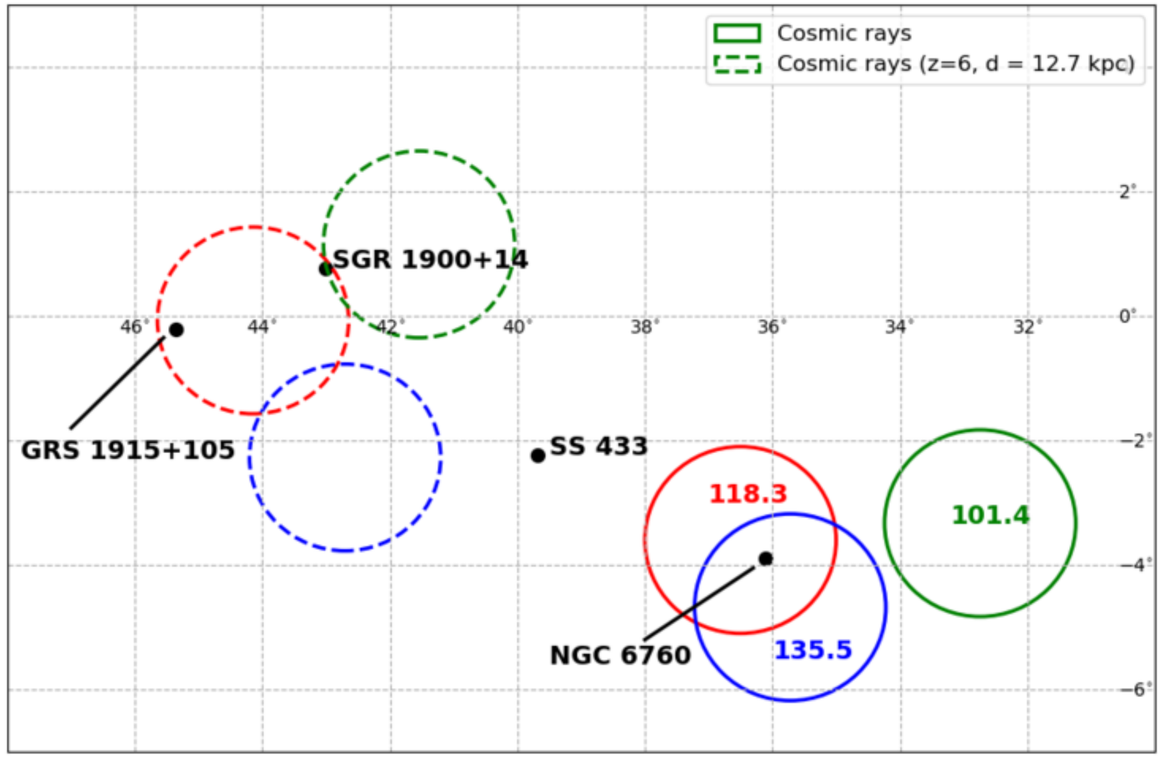

V.V., Hnatyk B., Hnatyk R., Zhdanov V., PoS(ICRC2021)672

Possible sources of the triplet

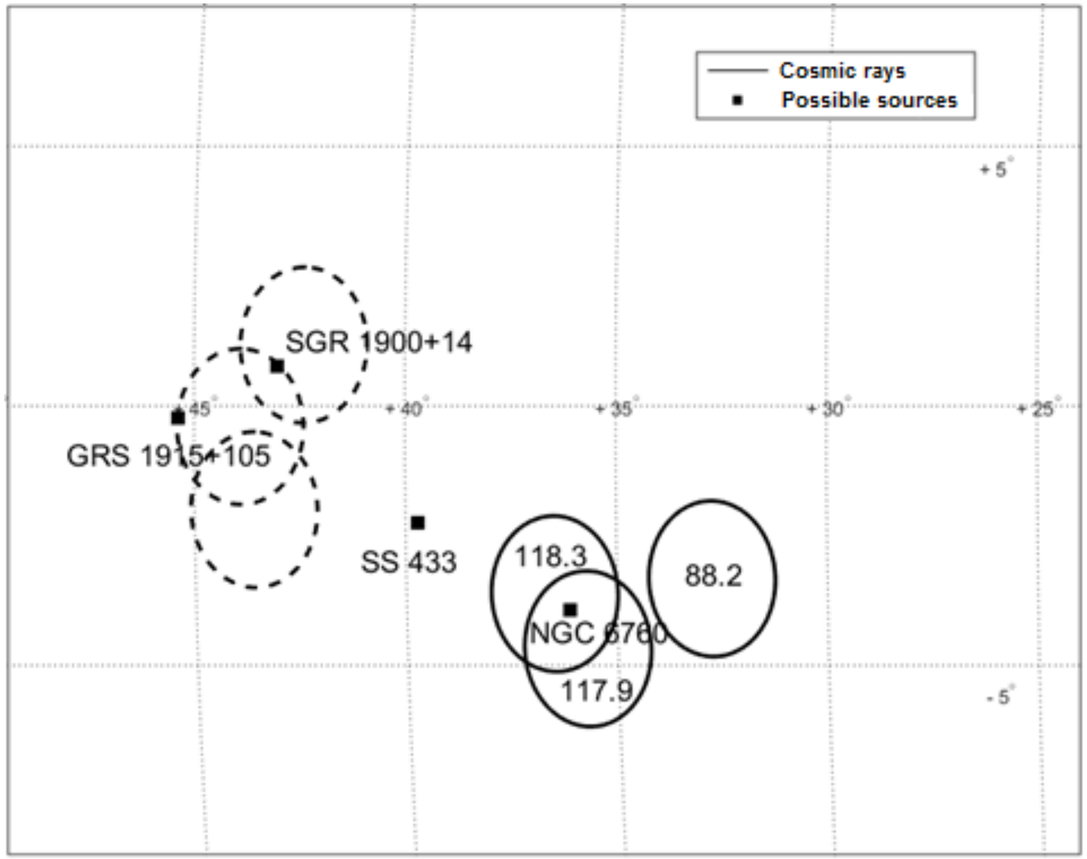

№	Name	Type	*l*, deg	*b*,deg	*d*, kpc
1	GRS 1915+105	Microquasar	45.37	-0.22	8.6±2.0
2	SS 433	Microquasar	39.69	-2.24	5.5±0.2
3	NGC 6760	Globular cluster	36.11	-3.9	7.4±0.4
4	SGR 1900+14	Magnetar	43.02	0.77	12.5±1.7

Solid circles - initial positions of CRs in the triplet with 1 sigma errors

Dashed circles - positions of CRs (Z=6) at the distance 12.5 kpc from the Earth

Magnetar SGR1900+14 is the most promising potential source

Magnetar SGR 1900+14

SGR1900+14 in IR band

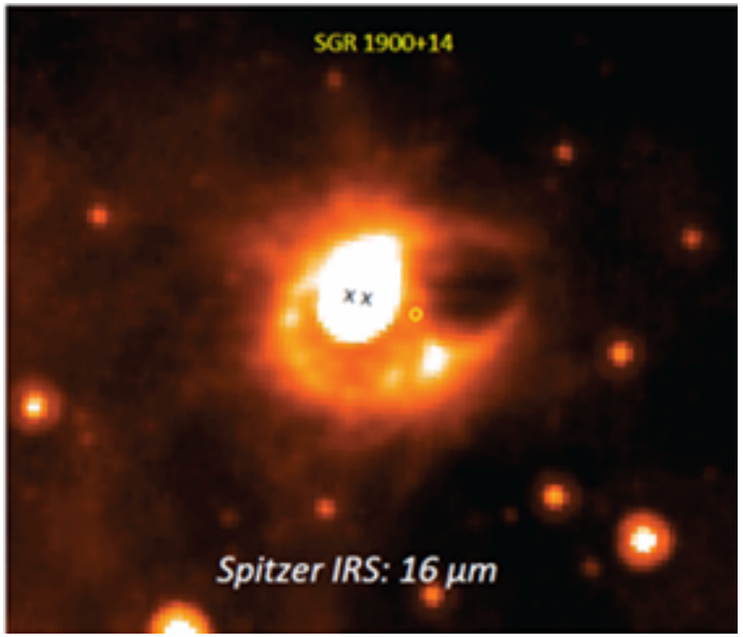

Magnetars - neutron stars with relatively large rotational periods (2... 8 s) and magnetic fields of the order of 10^{14} . . . 10^{15} G.

It is believed that newborn magnetars with millisecond rotation periods generate a powerful relativistic pulsar wind, whose shock waves can accelerate cosmic rays to energies of the order of EHECR energy of 10^{20} eV and more.

Artists picture of the magnetar

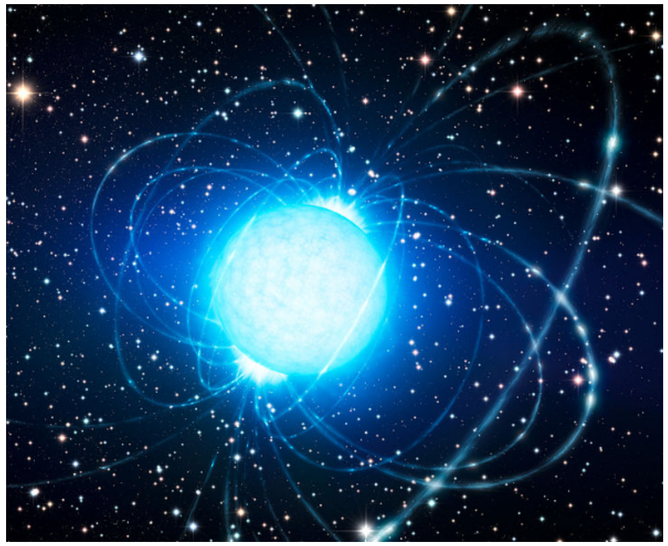

Magnetar SGR1900+14: P=5.2 s, $B = 4 \times 10^{14}$ G, d = 12.5 kpc

Giant magnetar flares

Some magnetars, including the magnetar SGR 1900+14, can produce giant flares of gamma-ray emission (SGR 1900+14 flared on 27th August, 1998).

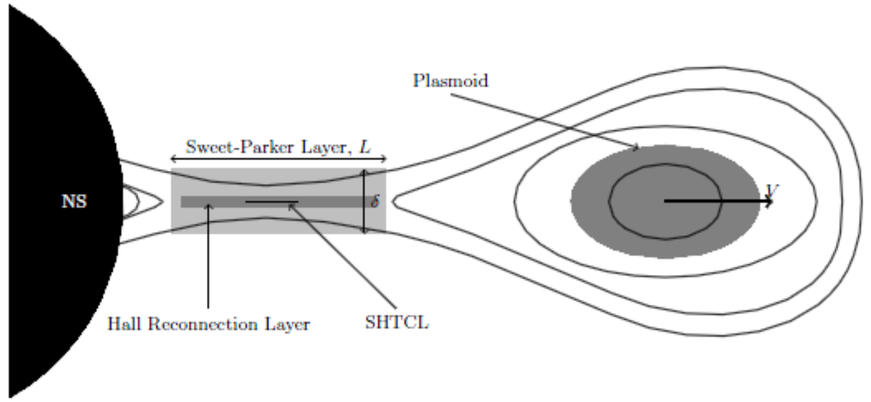

Figure 1. This figure displays the setup of the different reconnecting current layers. The macroscopic Sweet-Parker layer with length $L \sim 10^5$ cm and width $\delta \sim 0.01$ cm is the largest of the three. This layer is then thinned down vertically as strong magnetic flux is convected into the dissipation region. The Hall reconnection layer, represented by the dark gray region, develops when δ becomes

Aharonian et al. 2012

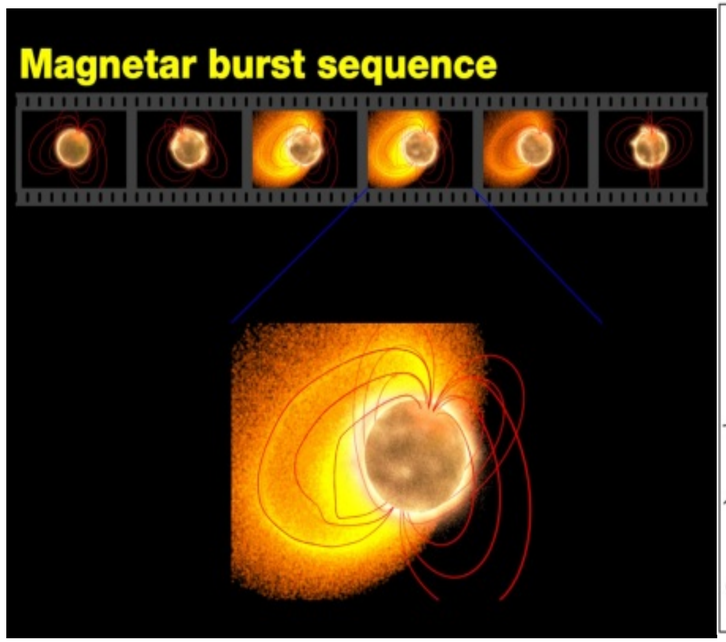

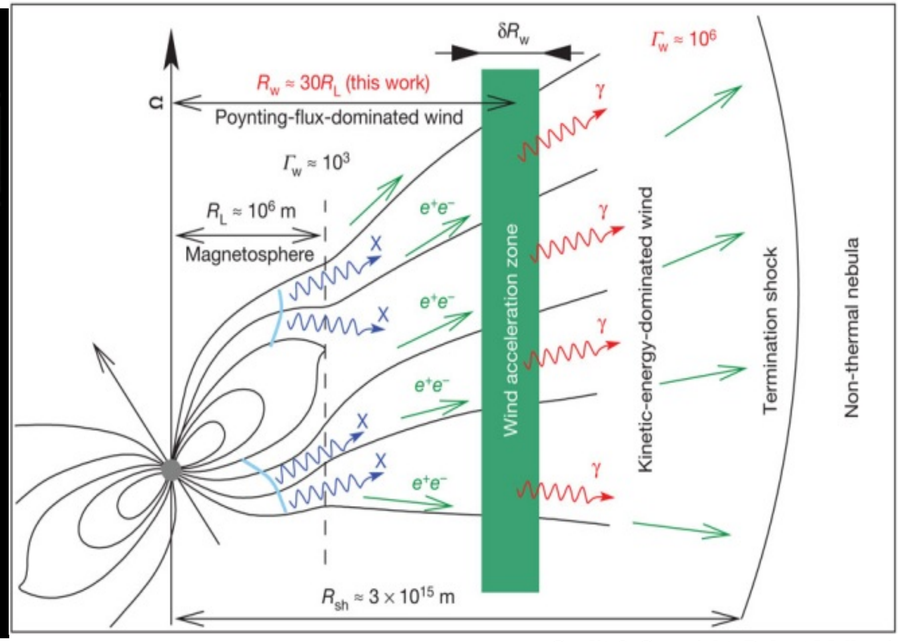

Credit & Copyright: Robert Mallozzi

Maximum accessible proton energy $E_{p,max}$ in a flaring source, with bulk Lorentz factor $\Gamma = 10$

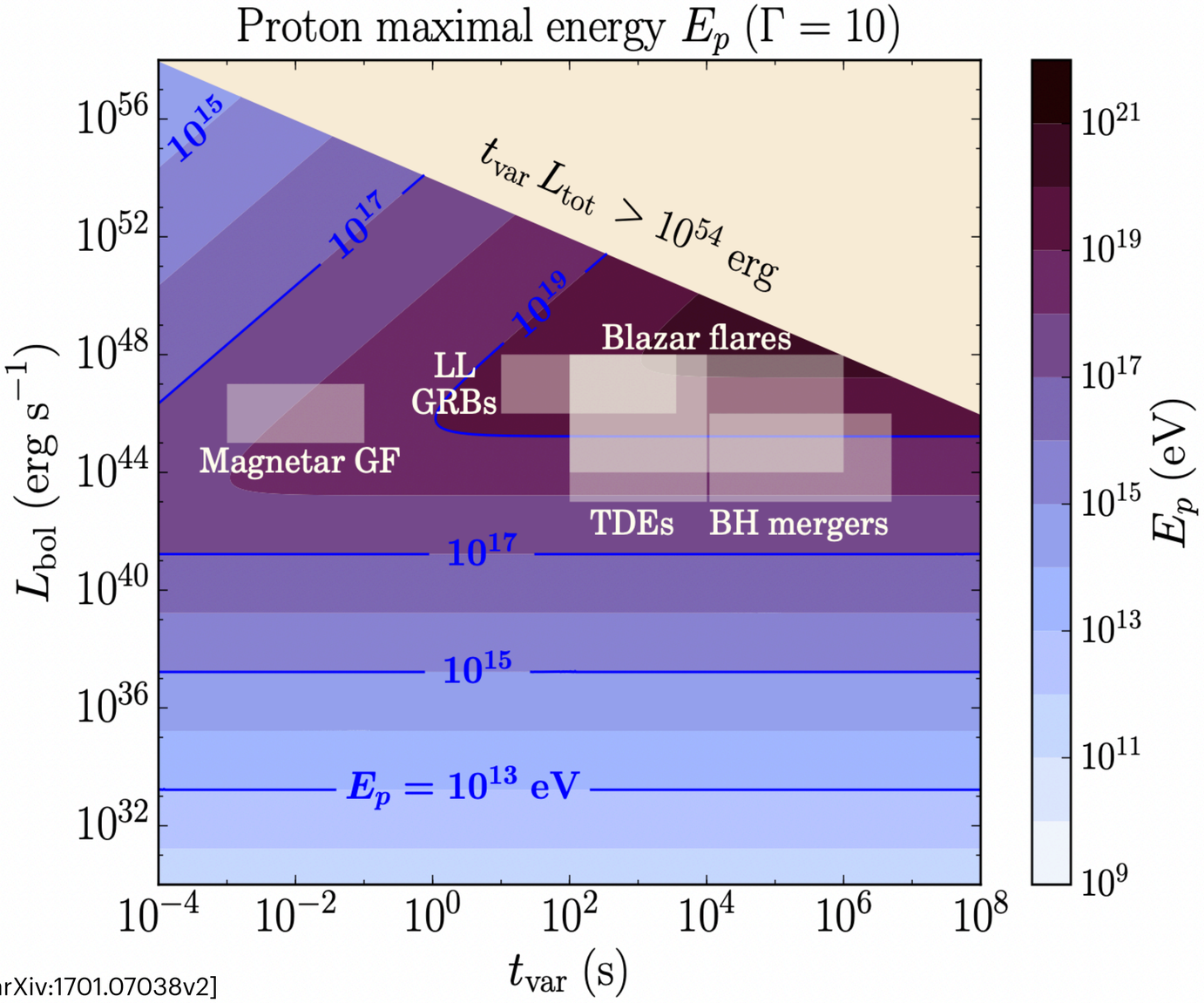

[arXiv:1701.07038v2]

In case of SGR1900+14,

max acceleration energy

$$E_{max} = Z \times E_{p,max} > 10^{20}\ \text{eV}$$

for nuclei with $Z > 10$

SGR1900+14 region

- 4FGL J1908.6+0915e
- H.E.S.S HOTS J1907+091
- HAWC 3HWC J1907+085
- SNR G42.8+0.6
- SNR G43.3-00.2

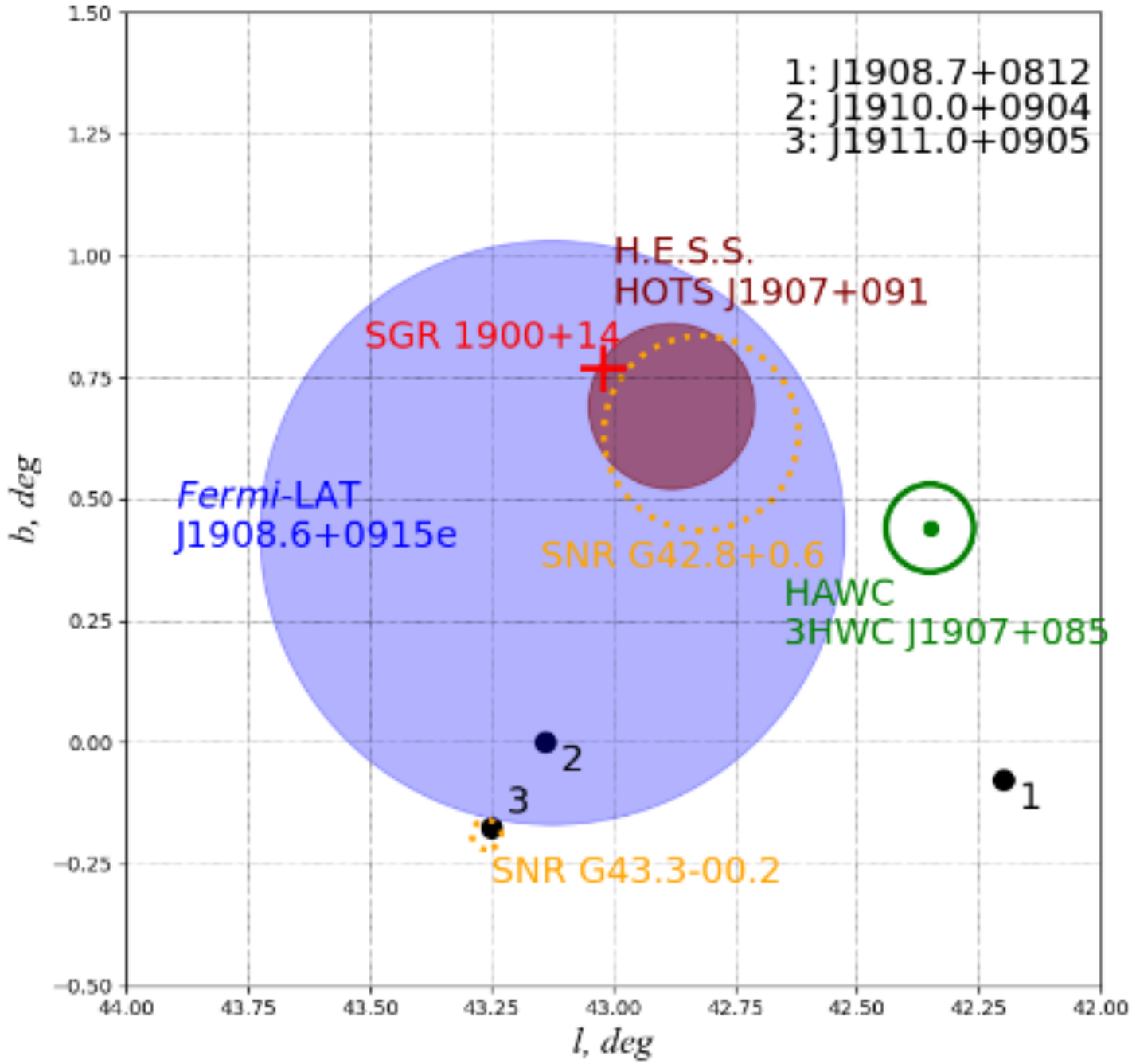

V.V., Hnatyk B., Hnatyk R., Zhdanov V., PoS(ICRC2021)672

Multiwavelength observations of SGR1900+14

Radio

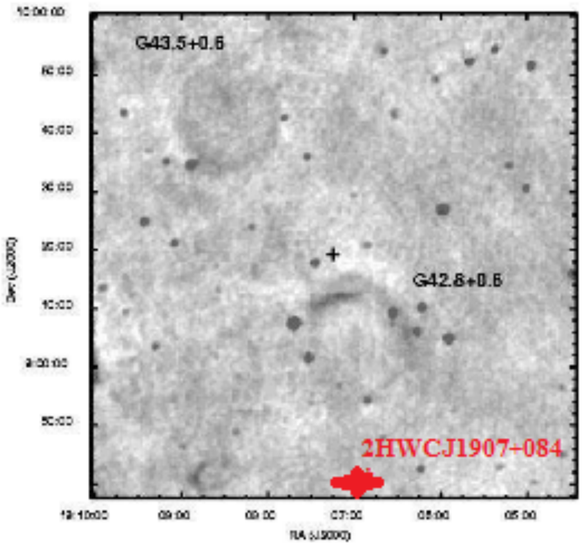

Kaplan et al, ApJ 566(2002)

Optical

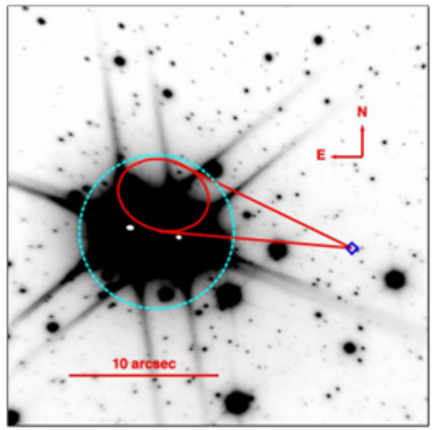

FIG. 9.— The position of the putative counterpart of SGR 1900+14 (blue diamond) traced back by 6 kyr is marked by the solid ellipse (red in the online version). The size of the ellipse denotes the positional uncertainty corresponding to the uncertainty in the proper motion measurement. The solid (red) lines represent the 1-σ limits on the angle of motion. The dashed circle (cyan in the online version) denotes the cluster of massive stars (Vrba et al. 2000).

Tendulkar et al, ApJ 761 (2012)

IR

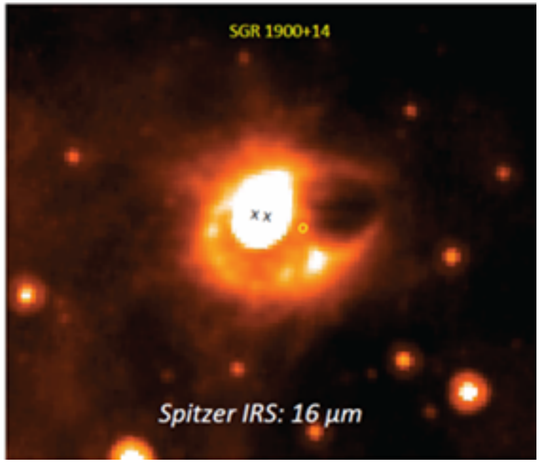

Natale G et al. ApJ837(2017)

X-ray NuSTAR 3-78 keV

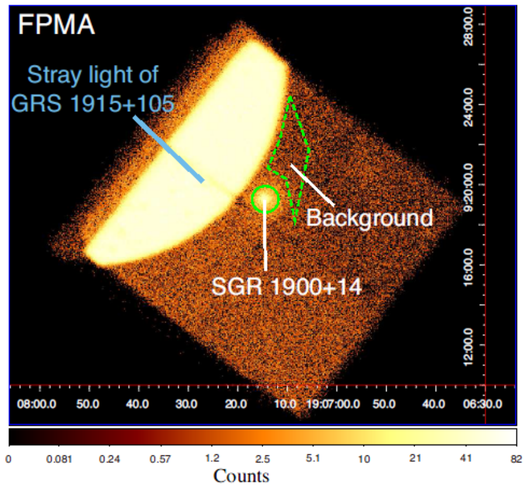

Tamba et al, PASJ 71(2019)

Fermi-LAT (100 MeV - 1 TeV)

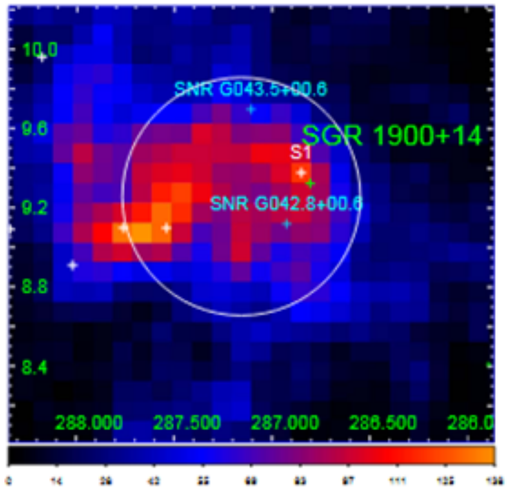

Li et al. ApL 835(2017)

HAWC (1-100 TeV)

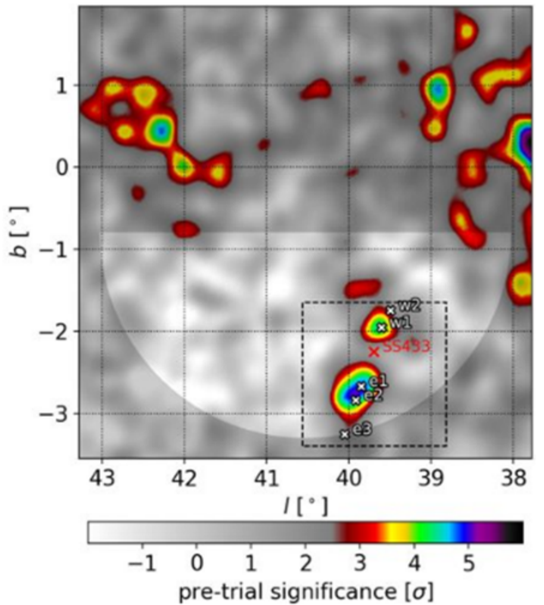

Our model of SGR1900+14 evolution

arXiv:2009.06081,
PoS(ICRC2021)672

1. Birthplace: 17 Myr ago in young stellar cluster Cl1900+14 d=12.5 kpc

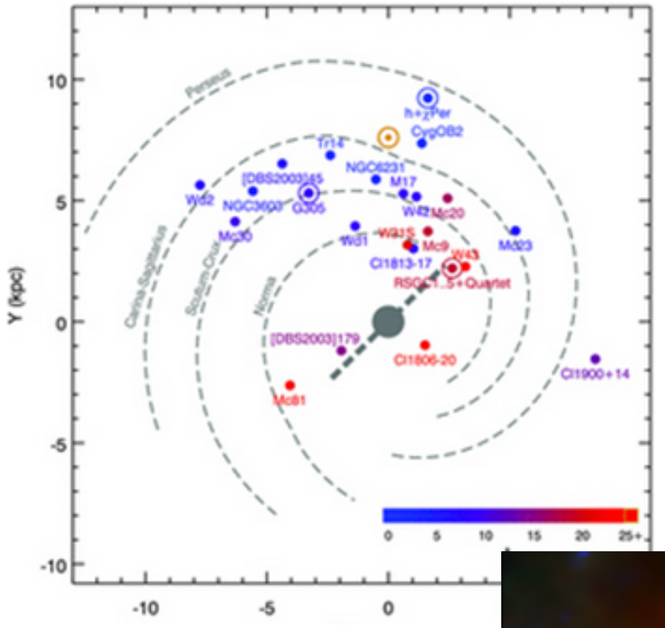

2. Explosion as SN Ic in stellar wind cavity

Newborn pulsar with P= 1ms and B = 4×10^{14} G

Magnetar with $E_{rot} \approx 10^{52}$ erg

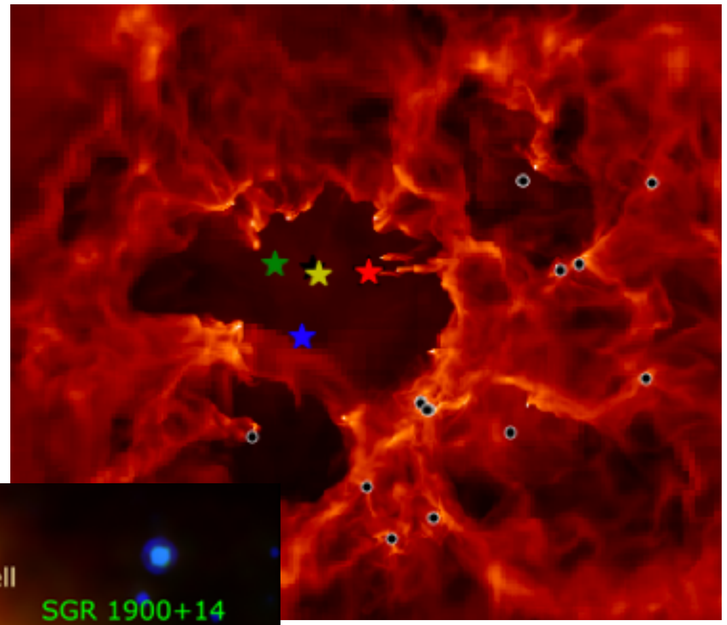

arXiv:1907.04316v1

E_{rot} was transformed into:

- $E_{ejecta} \leq 10^{52}$ erg (Hypernova model)
- $E_{MWN} \leq 10^{52}$ erg (magnetar wind nebula model)

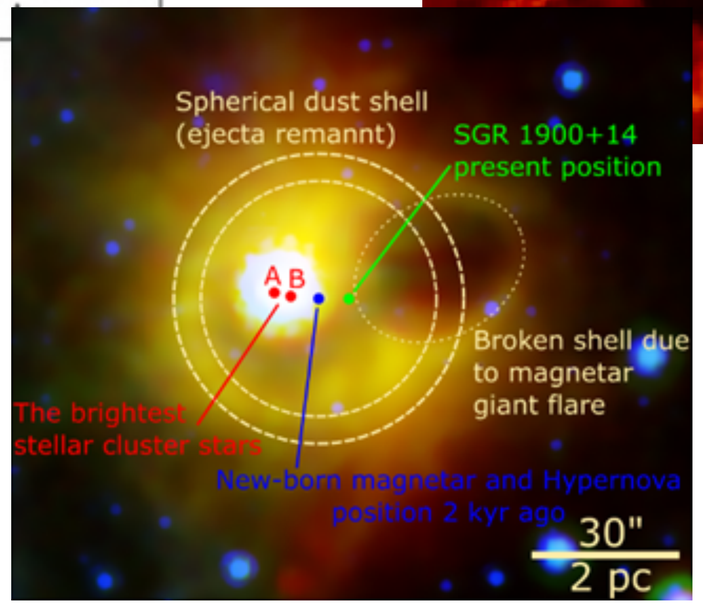

$2\ M_{sun}$ spherical dust shell-relic of SN shell

Broken shell is evaporated by collimated giant flare

PWN HESS J1825-137 at 4 kps
(SGR1900+14- twin)

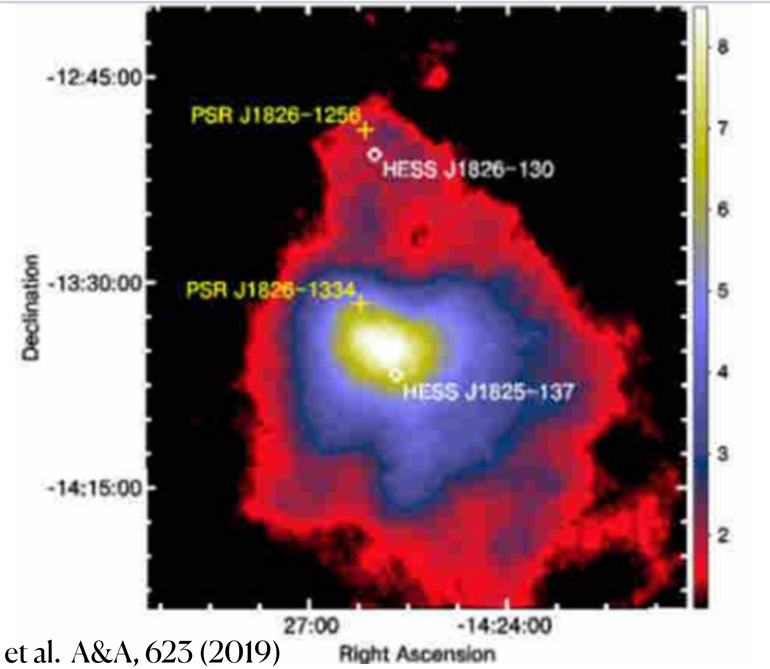

Duvidovich et al. A&A, 623 (2019)

Evolution of the magnetar driven Hypernova/MWN

$$E_{ejecta} = 10^{51}\,\text{erg}, \quad E_{mag\_wind} = E_{rot} = 10^{52}\text{erg}$$

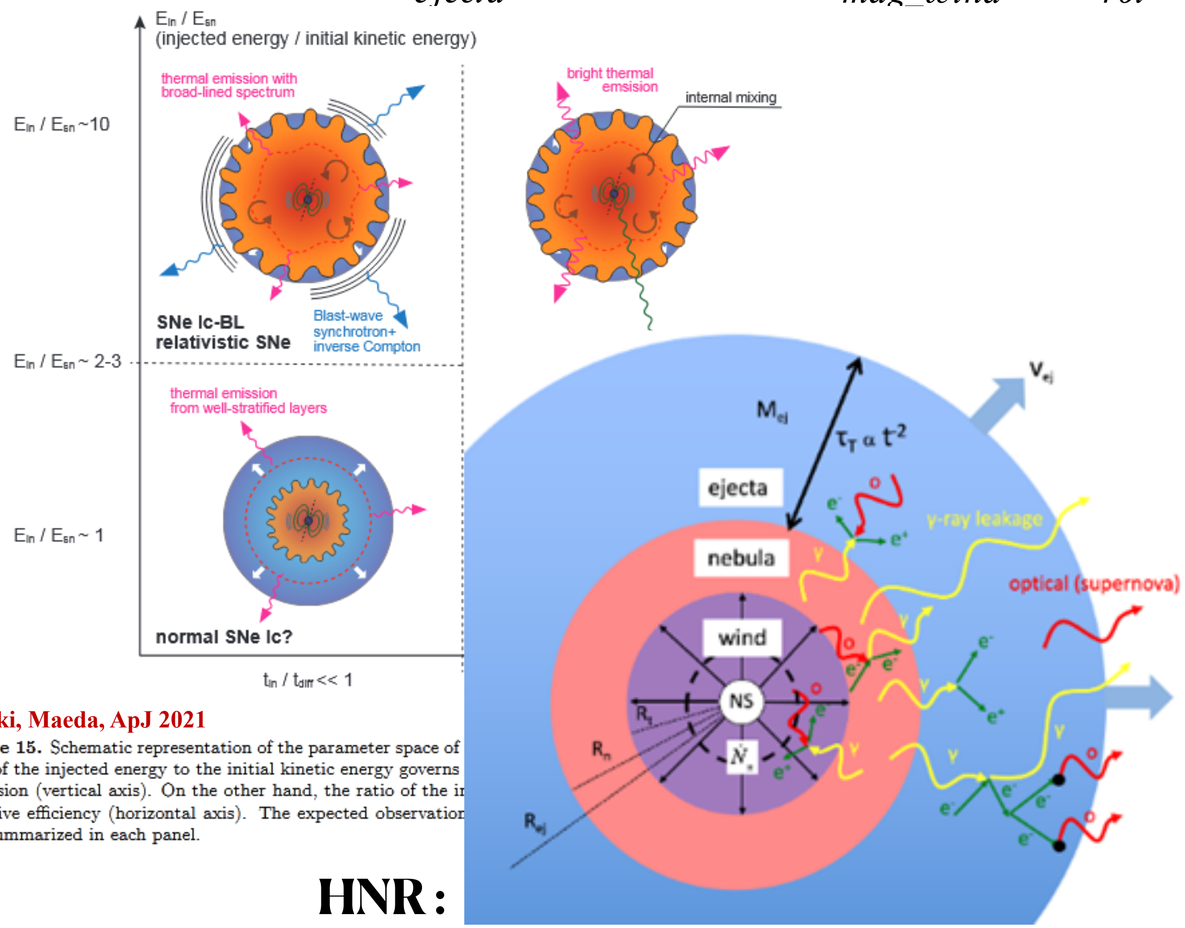

Suzuki, Maeda, ApJ 2021

Figure 15. Schematic representation of the parameter space of ratio of the injected energy to the initial kinetic energy governs expansion (vertical axis). On the other hand, the ratio of the ir radiative efficiency (horizontal axis). The expected observation also summarized in each panel.

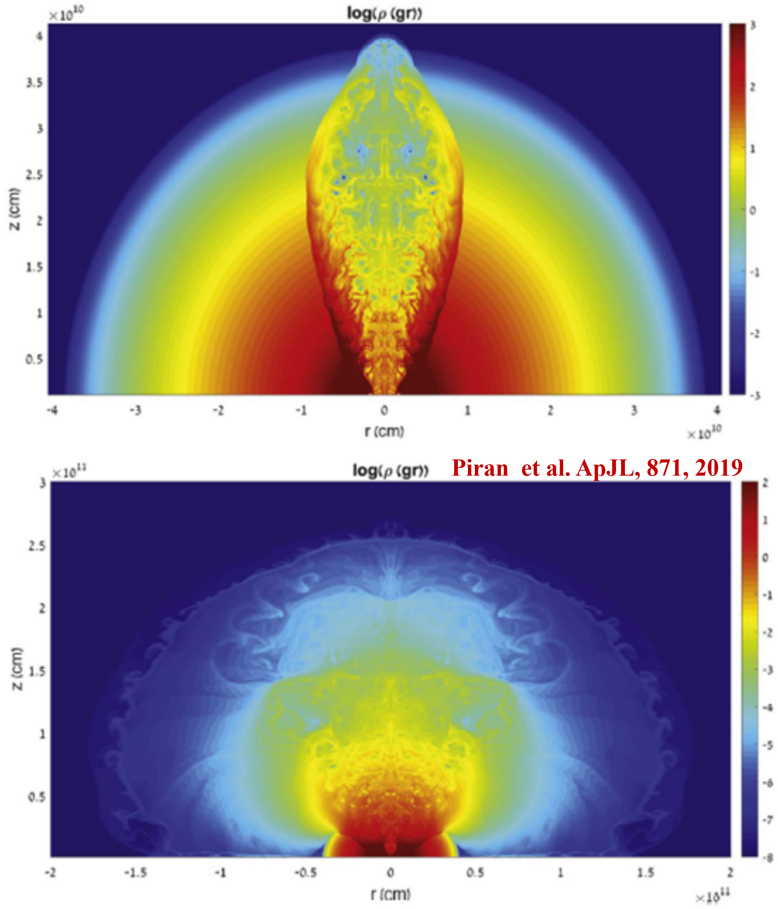

Piran et al. ApJL, 871, 2019

HNR:

Magnetar Wind Nebula (MWN) pressure protrudes dense internal part of ejecta and accelerates its external layers up to $E_{ejecta} = 10^{52}$ erg

Diffusive Shock Acceleration at HNR shock:

$E_{cr,p} = (3\text{-}5) \cdot 10^{50}$ erg, $E_{cr,e} = K_{ep} \times E_{cr,p} \sim 10^{48}$ erg

MWN:

Break out of collimated wind jet creates large-scale MWN (r ~ 30 pc) with $E_{MWN} \leq 10^{52}$ erg and $E_{cr,e+e-} \sim 10^{50}$erg ahead ejecta debris

(R=2-3 pc IR shell)

Spectral energy distribution modeling in case of HNR model

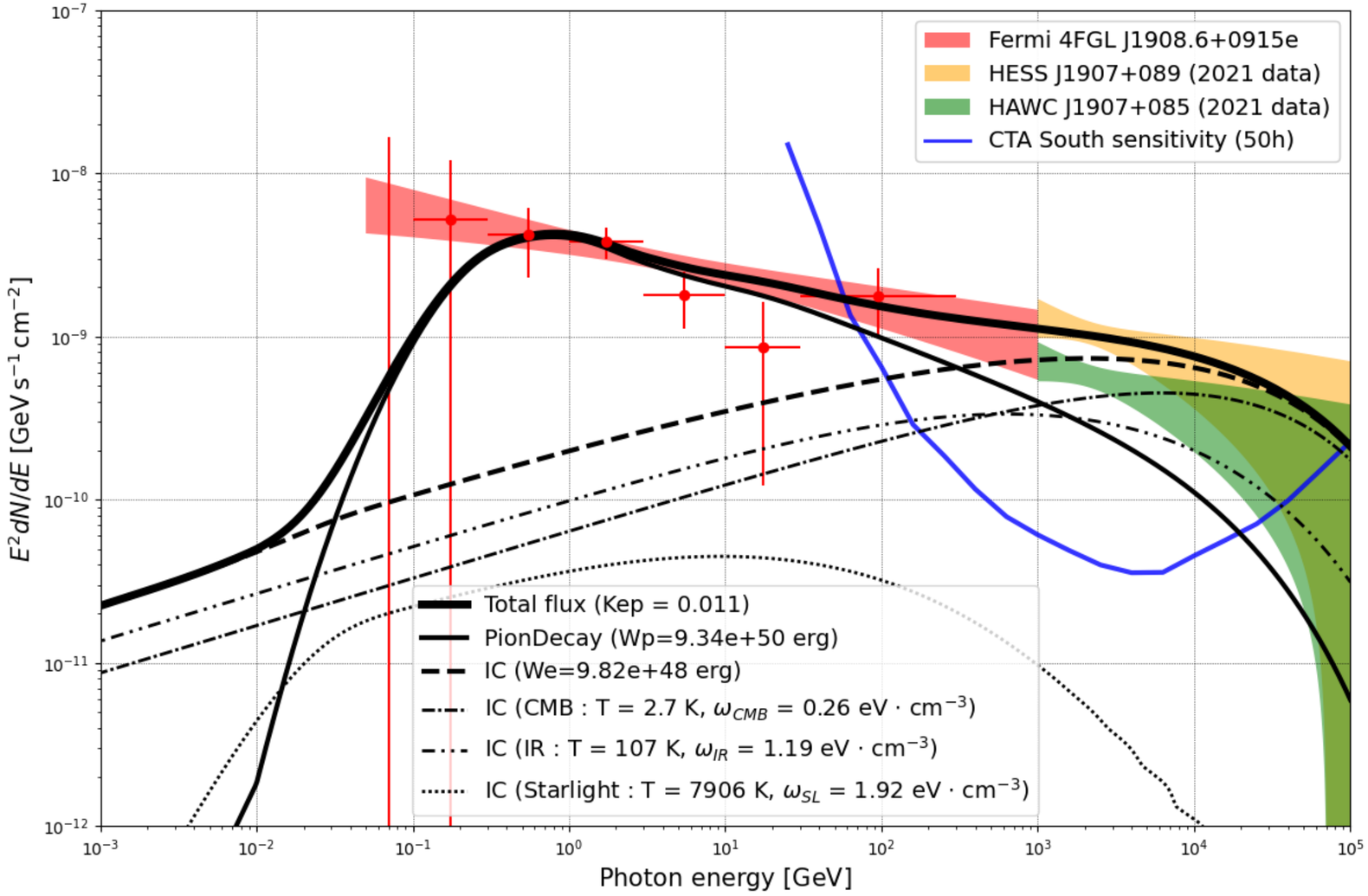

Best-fit spectrum corresponds to $W_p = 5 \times 10^{50} erg$, $K_{ep} = 0.004$

Spectral energy distribution modelling in case of MWN model with ECBPL lepton spectrum

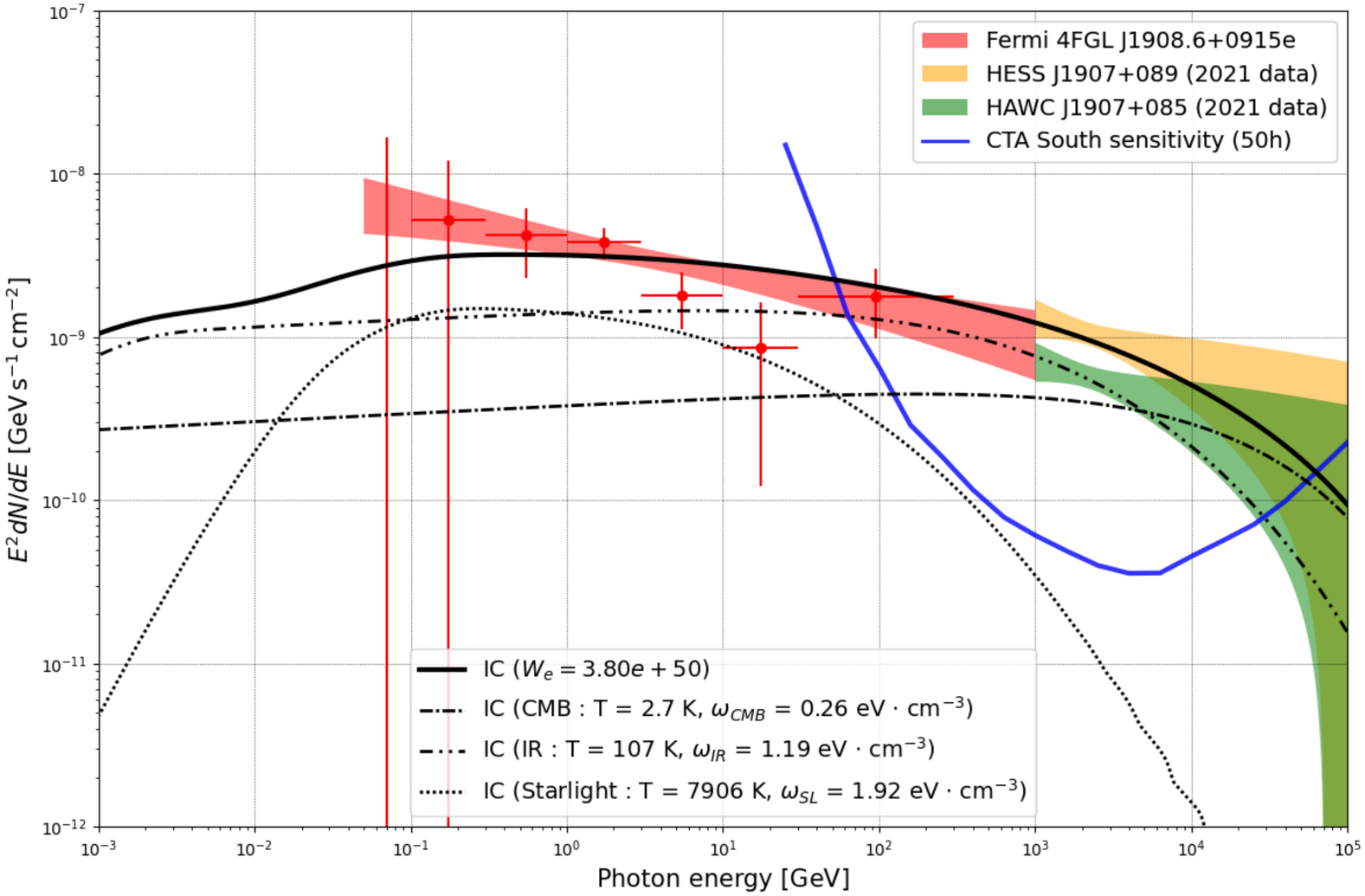

Best-fit spectrum corresponds to $W_e = 3.6 \times 10^{50}$ erg

PARAMETERS OF HNR AND MWN MODELS OF GAMMA-RAY EMISSION FROM SGR1900+14 OUTSKIRTS

Table 1: HNR and MWN NAIMA-fitted models of SED from SGR 1900+14 neighbourhood

2*Parameter	HNR: PL and ECPL spectra (i=p)		MWN: ECBPL(i=e)	MWN:Two electron population spectra (i=e)	
	PL	ECPL	ECBPL	ECPL #1	ECPL #2
E_{min} [GeV](fixed)	1	1	1	1	1
E_{max} [GeV](fixed)	1e6	1e6	1e6	1e6	1e6
$N_{0,i}$ [1/ eV]	(1.18±0.04)e35	(1.42±0.05)e37	(1.90±0.12)e40	(4.41±0.51)e38	(8.81±0.44)e34
$E_{0,i}$ [TeV]	3.93±0.1	0.78±0.01	0.19±0.01	1.91±0.19	1.81±0.19
$E_{br,i}$ [TeV]	-	-	0.0047±0.0003	-	-
$E_{cut,i}$ [TeV]	-	185.2±9.5	396.7±41.7	0.0096±0.0008	9.99±1.06
$\gamma_{1,i}$	2.55±0.01	2.41±0.03	1.49±0.07	1.65±0.11	-
$\gamma_{2,i}$	-	-	3.04±0.06	-	2.58±0.17
W_p [erg]	5.03e50	5.12e50	-	-	-
W_e [erg]	1.04e49	2.16e48	3.60e50	5.20e50	6.08e49
n_H [cm^{-3}]	11.42±0.66	9.81±0.35	-	-	-
K_{ep}	0.02 (fixed)	0.0041±0.0002	-	-	-

In both HNR and MWN cases the TeV gamma-ray emission corresponds to CR energy $E_{CR} \approx 5 \cdot 10^{50}$ erg in both hadronic (HNR) and leptonic (MWN) scenarios
Such CR energies are expected in Hypernova model of magnetar-related Supernova

Summary

The most promising candidates for UHECR accelerators are Hypernovae with millisecond pulsar/ magnetar, giant flares of magnetars, Kilonovae (NS-NS mergers), tidal disruption events etc. accompanied by (mildly) relativistic jets with close to the Earth directions.

Galactic magnetar SGR1900+14 may be responsible for the observed EHECR triplet

Promising signature of effective acceleration processes in magnetars' neighbourhoods should be nonthermal high-energy and very high-energy gamma-ray emission

We have explained the observed gamma-ray emission from the magnetar SGR 1900+14 neighbourhood in a model of magnetar-connected HNR and MWN created by an energy supply to a SN ejecta from a fast-rotating newborn magnetar with initial rotational energy $E_{rot} \sim 10^{52}$ erg

THANK YOU!

back up

The era of multi-messenger astronomy

Multi-messenger carriers:

- Cosmic rays (CR, protons, nuclei leptons)
- Neutrinos
- EM radiation (gamma-rays etc.)
- Gravitational waves

CR are the principal, because:

Interaction of accelerated particles (CR) with magnetic fields and EM background results in generation of nonthermal emission and neutrinos

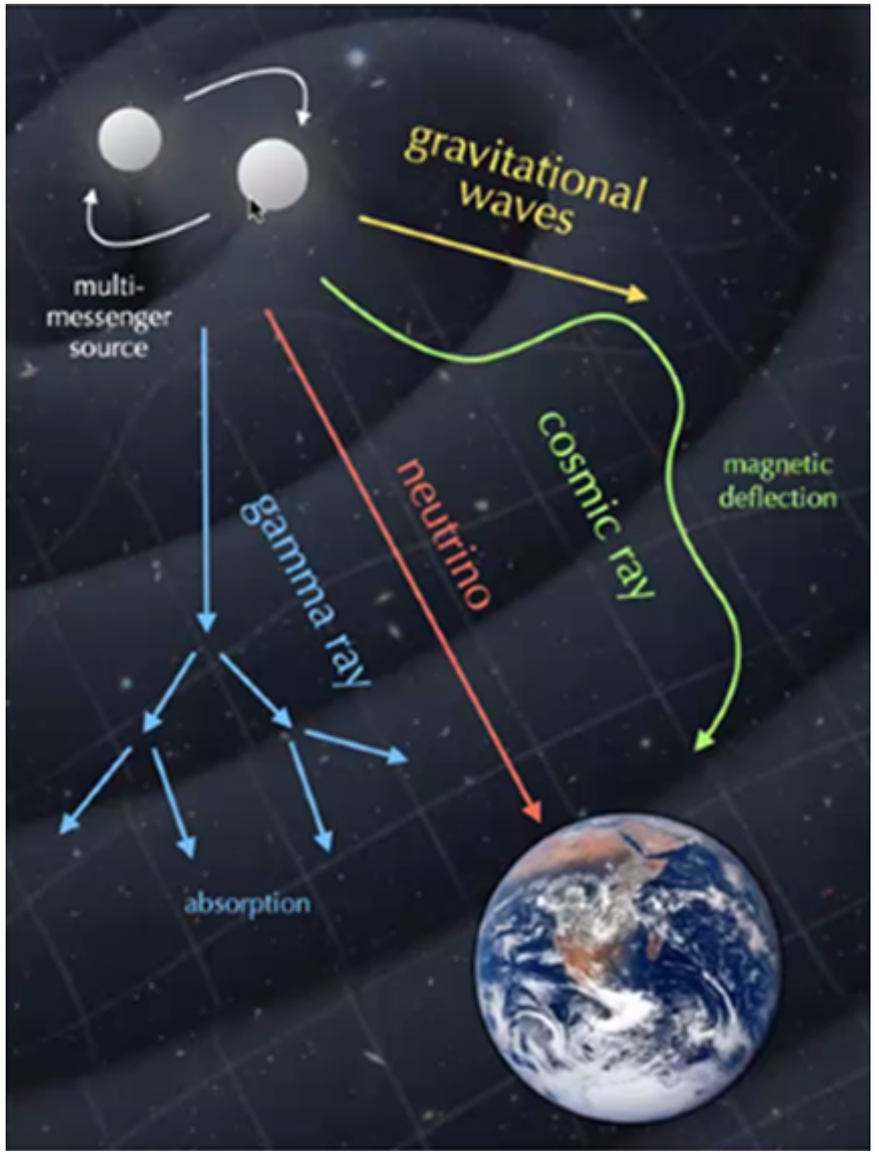

First steps in multi-messenger astronomy

Coordinates: 13h 09m 48.08s, −23° 22′ 53.3″

GW170817

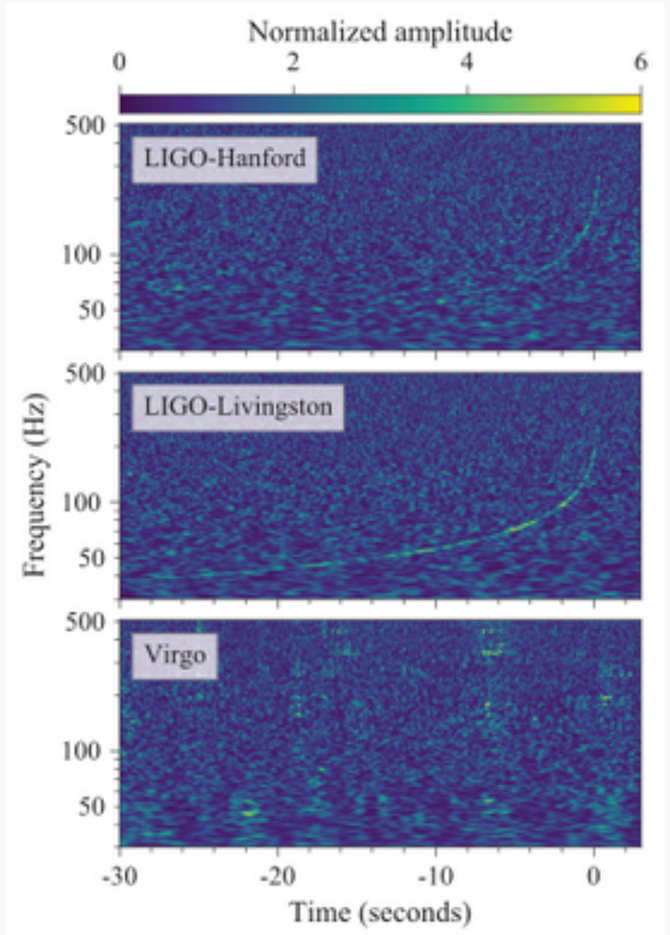

The GW170817 signal as measured by the LIGO and Virgo gravitational wave detectors

Neutron_star_collision.ogv

(1)

NS-NS merger:
kilonova:
gravitational waves + short GRB

Coordinates: 13h 09m 47.2s, −23° 23′ 4″

NGC 4993

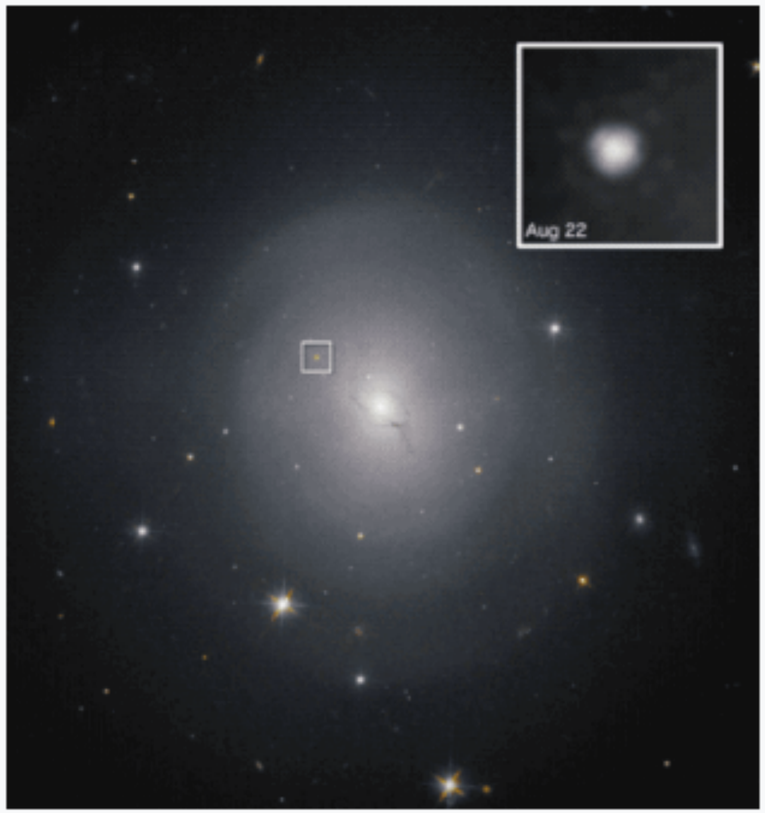

NGC 4993 and GRB 170817A afterglow as taken by Hubble Space Telescope[1]

Multimessenger observations of a flaring blazar coincident with high-energy neutrino IceCube-170922A

The IceCube Collaboration, *Fermi*-LAT, MAGIC, *AGILE*, ASAS-SN, HAWC, H.E.S.S., *INTEGRAL*, Kanata, Kiso, Kapteyn, Liverpool Telescope, Subaru, *Swift/NuSTAR*, VERITAS, and VLA/17B-403 teams*†

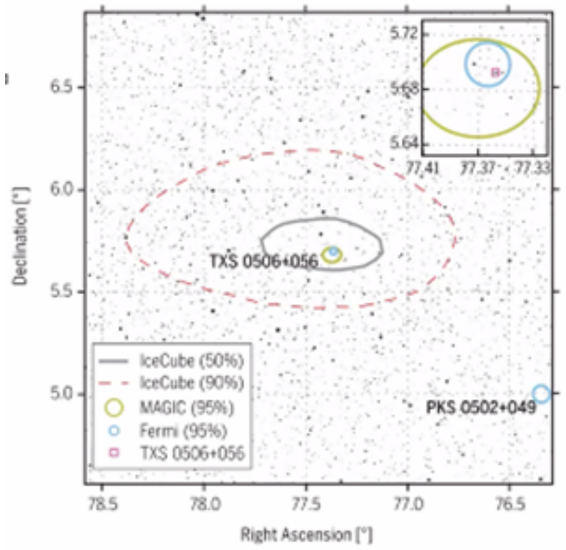

Multimessenger observations of blazar TXS 0506+056. The 50% and 90% containment regions for the neutrino IceCube-170922A (dashed red and solid gray contours, respectively), overlain on a V-band optical image of the sky. Gamma-ray sources in this region previously detected with the *Fermi* spacecraft are shown as blue circles, with sizes representing their 95% positional uncertainty and labeled with the source names. The IceCube neutrino is coincident with the blazar TXS 0506+056, whose optical position is shown by the pink square. The yellow circle shows the 95% positional uncertainty of very-high-energy γ-rays detected by the MAGIC telescopes during the follow-up campaign. The inset shows a magnified view of the region around TXS 0506+056 on an R-band optical image of the sky.

The IceCube Collaboration *et al.*, *Science* **361**, 146 (2018) 13 July 2018

(2)
Blazar flare: gamma-rays+neutrino

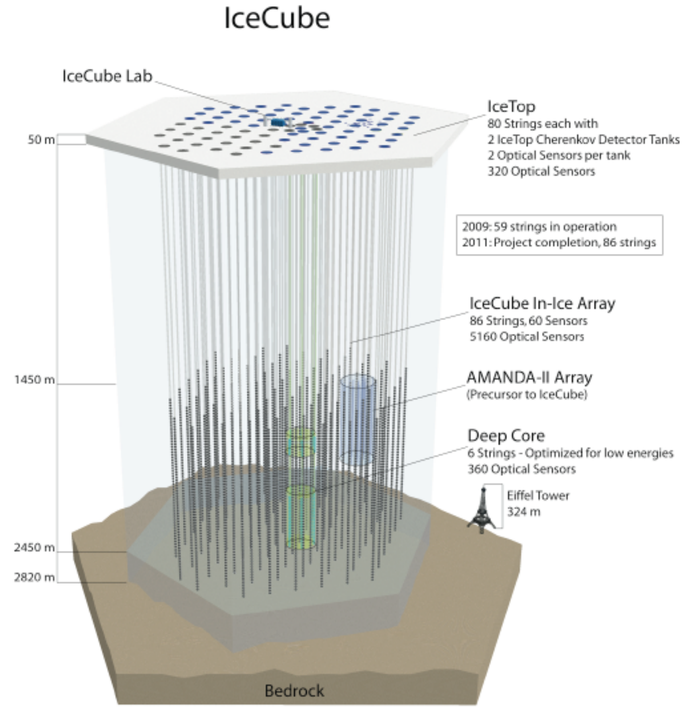

[IceCube, PoS (ICRC2019) 1021]

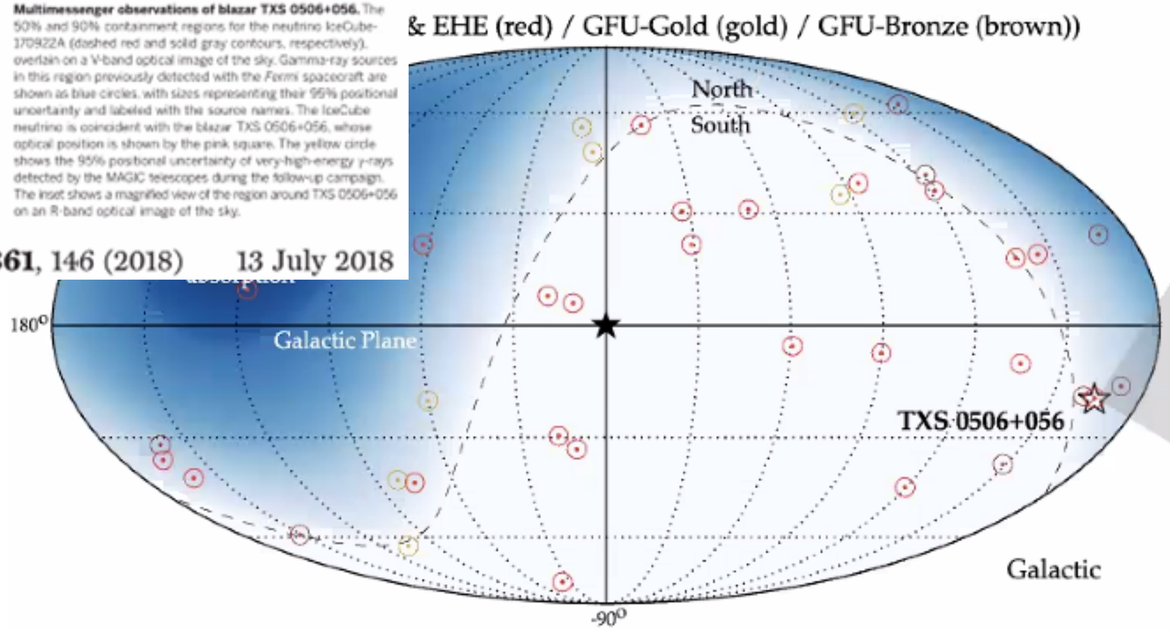

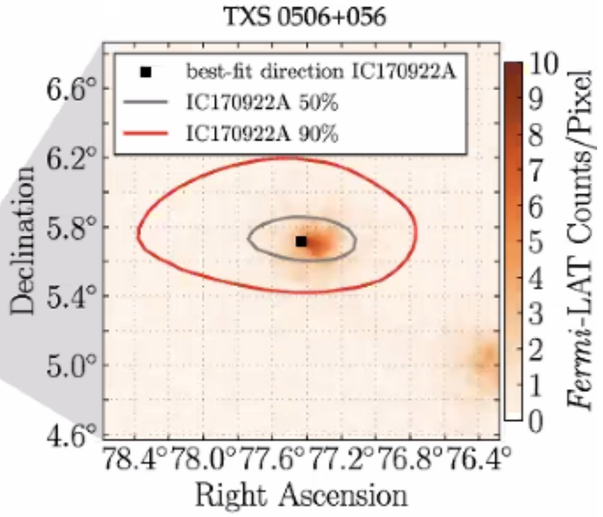

Multi-messenger carriers: photons, neutrinos, CR + (gravitational waves)

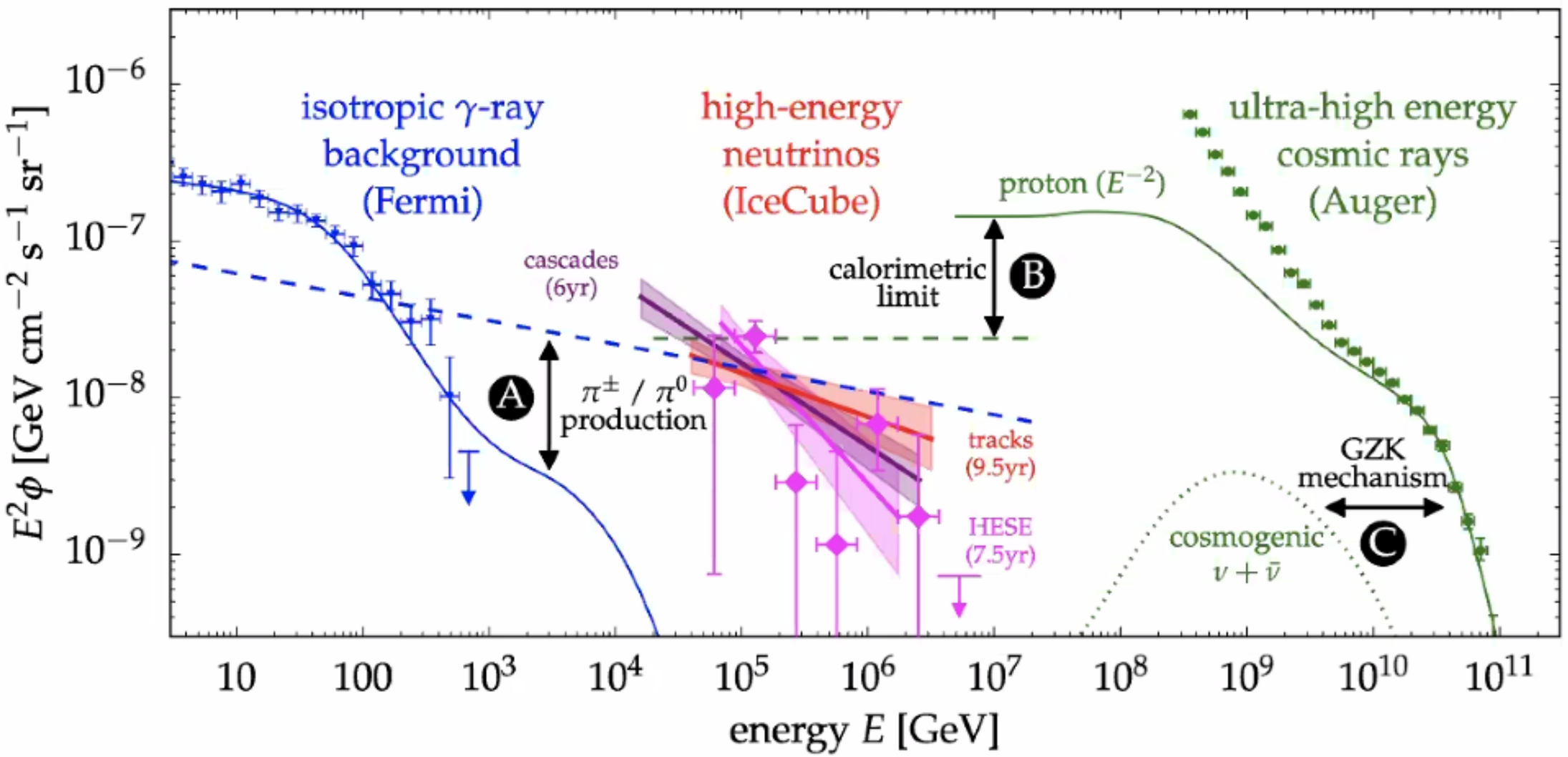

Ahlers and Halzen, arXiv:1805.11112v1

Variant 2: protrusion of SN ejecta due to CD instability

3D HD simulations of SN ejecta (10^{51} erg, $10 M_{sun}$)
with a central energy source 10^{52} erg = L(10^{46} erg/s) • t_c (10^6 s)

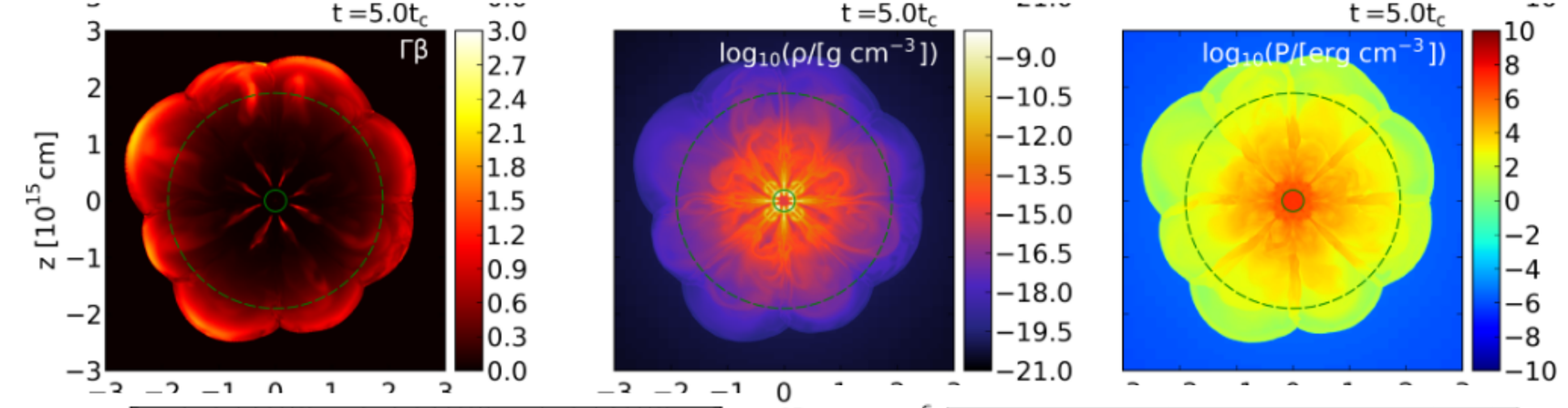

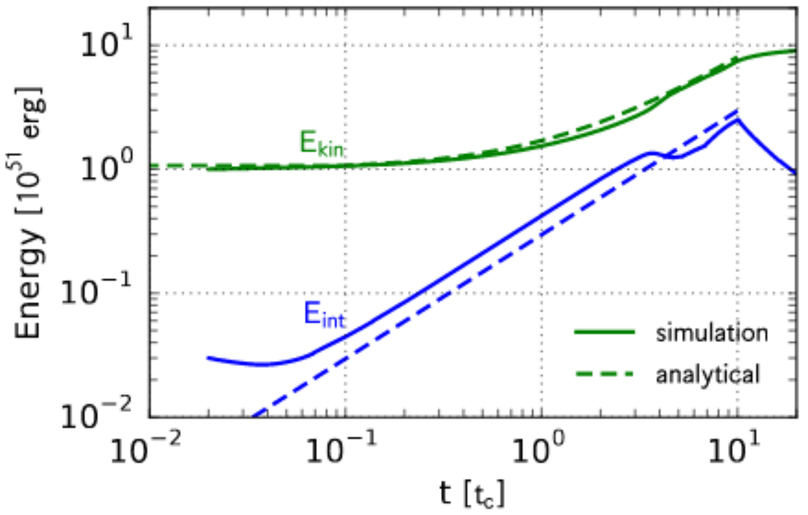

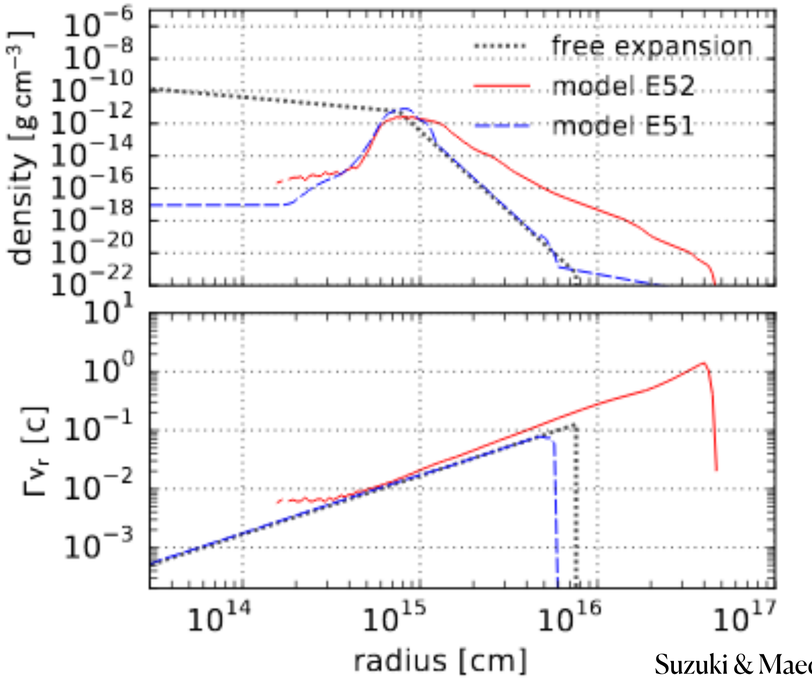

$t = 20 \cdot t_c = 20 \cdot 10^6$ sec

V ($10 M_{sun\_shell}$) x 2 kyr = 6 pc

cf. R_ ($5 M_{sun\_IR-shell}$) = 2 pc

Suzuki & Maeda, 2019Ap J...880..150S arXiv:1906.07381v1

Variant 1: Evolution of magnetar driven Hypernova

$(E_{ejecta} = 10^{51}\,\mathrm{erg},\ \ E_{mag\_wind} = E_{rot} = 10^{52}\,\mathrm{erg})$

CLASSICAL SITUATION: HNR
Magnetar Wind pressure accelerates ejecta

up to $E_{ejecta} = 10^{52}$ **erg**

Diffusive Shock Acceleration:

$$E_{cr,p} = (3-5)\times 10^{50}\ \text{erg}$$

$$E_{cr,e} \sim 10^{48}\ \text{erg}$$

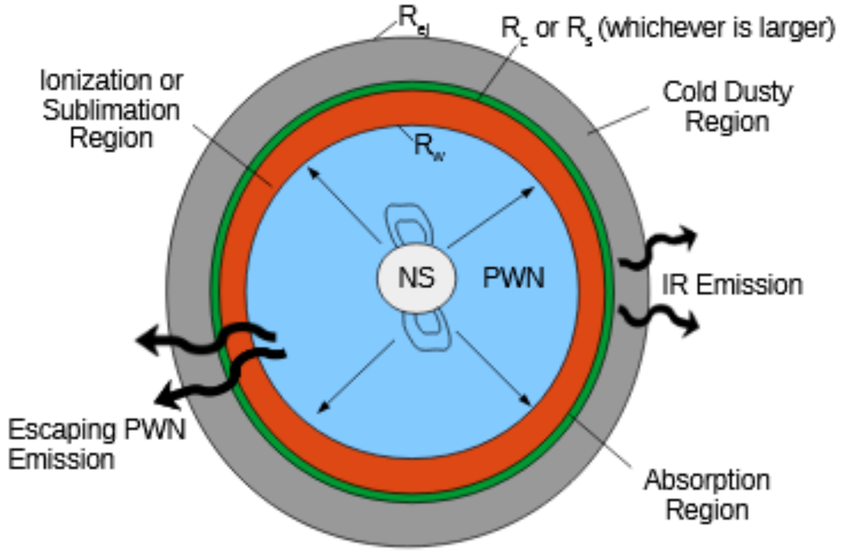

Energy Dominated MWN SITUATION:
large-scale MWN (r > 30 pc) with $E_{MWN} \leq 10^{52}$ **erg**

VARIANT 1: BREAK OUT OF COLLIMATED WIND JET
(Piran et al. 2020)

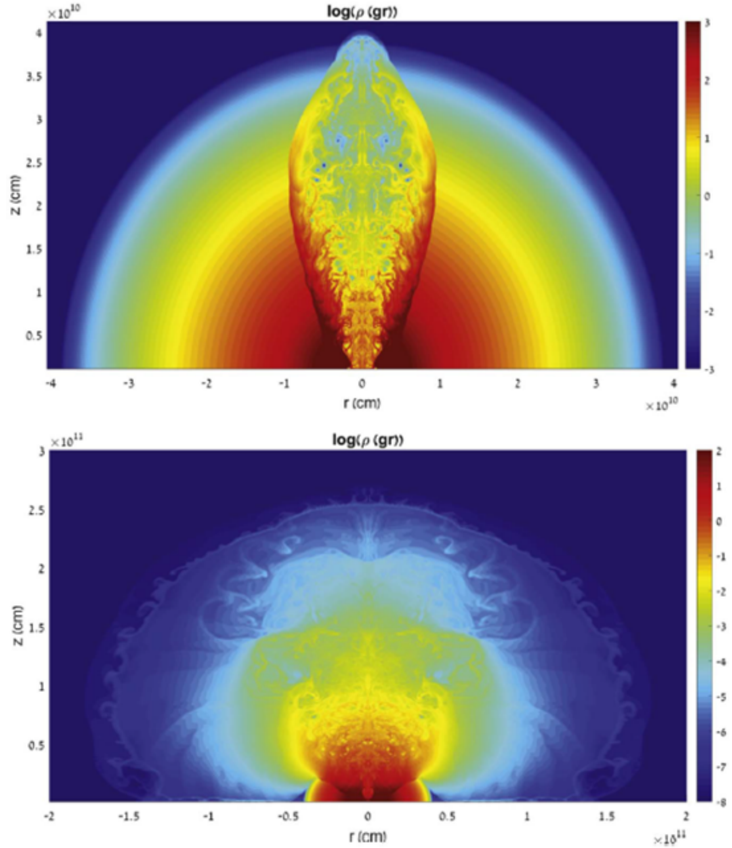

Spectral energy distribution modeling in case of HNR model

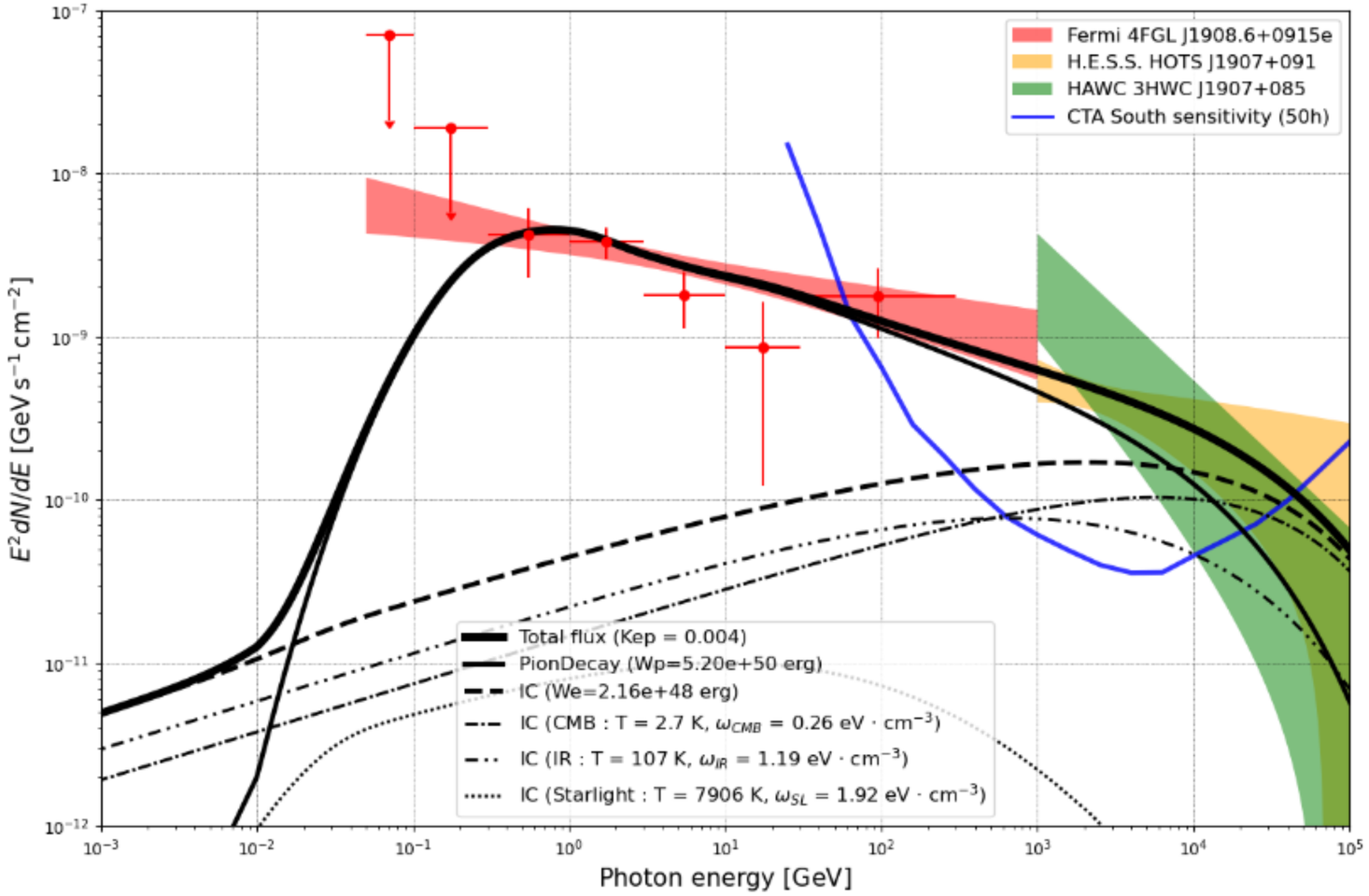

Best-fit spectrum corresponds to $W_p = 5 \times 10^{50} erg$, $K_{ep} = 0.004$

Spectral energy distribution modelling in case of MWN model with ECBPL lepton spectrum

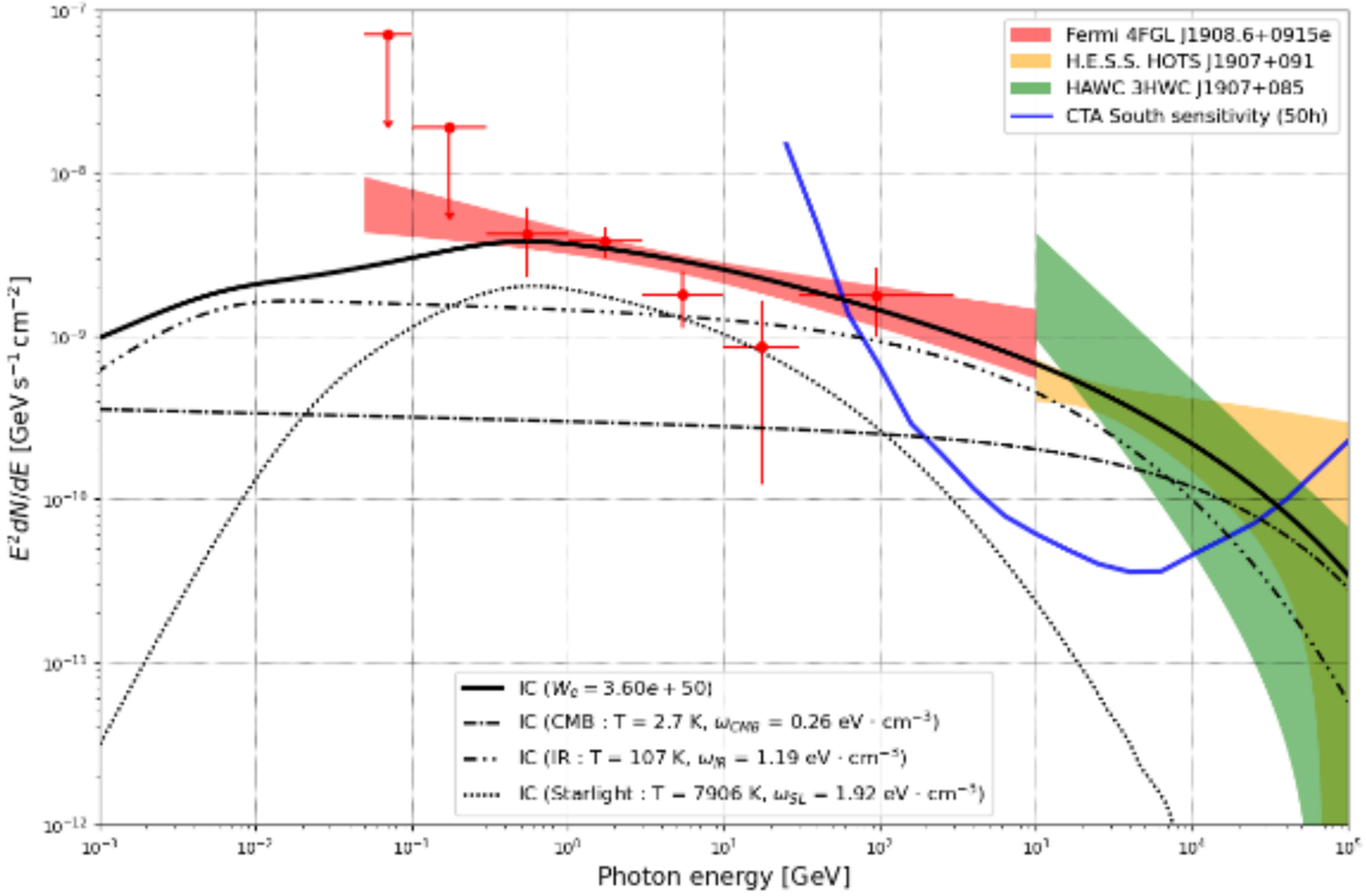

Best-fit spectrum corresponds to $W_e = 3.6 \times 10^{50}$ erg

Naima package

Naima is a Python package for computation of non-thermal radiation from relativistic particle populations. It includes tools to perform MCMC fitting of radiative models to X-ray, GeV, and TeV spectra.

Model:

1) Power law spectrum or power law spectrum with exponential cut-off

$$f(E) = A(E/E_0)^{-\alpha}$$

$$f(E) = A(E/E_0)^{-\alpha}\exp(-(E/E_{cut})^{\beta})$$

2) Pion decay, Inverse Compton, Synchrotron

3) Prior parameters for fitting: spectral index, A, E_0, E_{cut}, nh (for pion decay), B (for synchrotron)

Hadronic mechanism of emission

The main mechanism for the energy loss of protons and nuclei of the TeV-PeV bands in the ISM is the inelastic nucleon-nucleon (mainly proton-proton) collisions, as a result of which charged and neutral pions are born. The decay of the neutral pions into gamma-photon pairs completes the operation of the so-called hadronic mechanism of gamma-ray production.

$$p + p/\gamma \rightarrow p/n + \pi^{\pm} + \pi^{0} + K^{\pm} + \cdots$$

$$\begin{aligned}
\pi^{+} \rightarrow \quad & \mu^{+} + \nu_{\mu}, \\
& \mu^{+} \rightarrow e^{+} + \nu_{e} + \bar{\nu}_{\mu} \\
\pi^{-} \rightarrow \quad & \mu^{-} + \bar{\nu}_{\mu}, \\
& \mu^{-} \rightarrow e^{-} + \bar{\nu}_{e} + \nu_{\mu}, \\
\pi^{0} \rightarrow \quad & \gamma + \gamma \\
K^{\pm} \rightarrow \quad & \mu^{+}/\mu^{=} + \nu_{\mu}/\bar{\nu}_{\mu}
\end{aligned}$$

OUR MODEL: HYPERNOVA EXPLOSION IN CAVITY BLOWN BY THE WINDS OF STELLAR CLUSTER'S STARS

EVOLUTION of YOUNG STAR CLUSTER IN MOLECULAR CLOUD UP TO FIRST SN EXPLOSION (t=17 Myr in SGR1900 CASE)

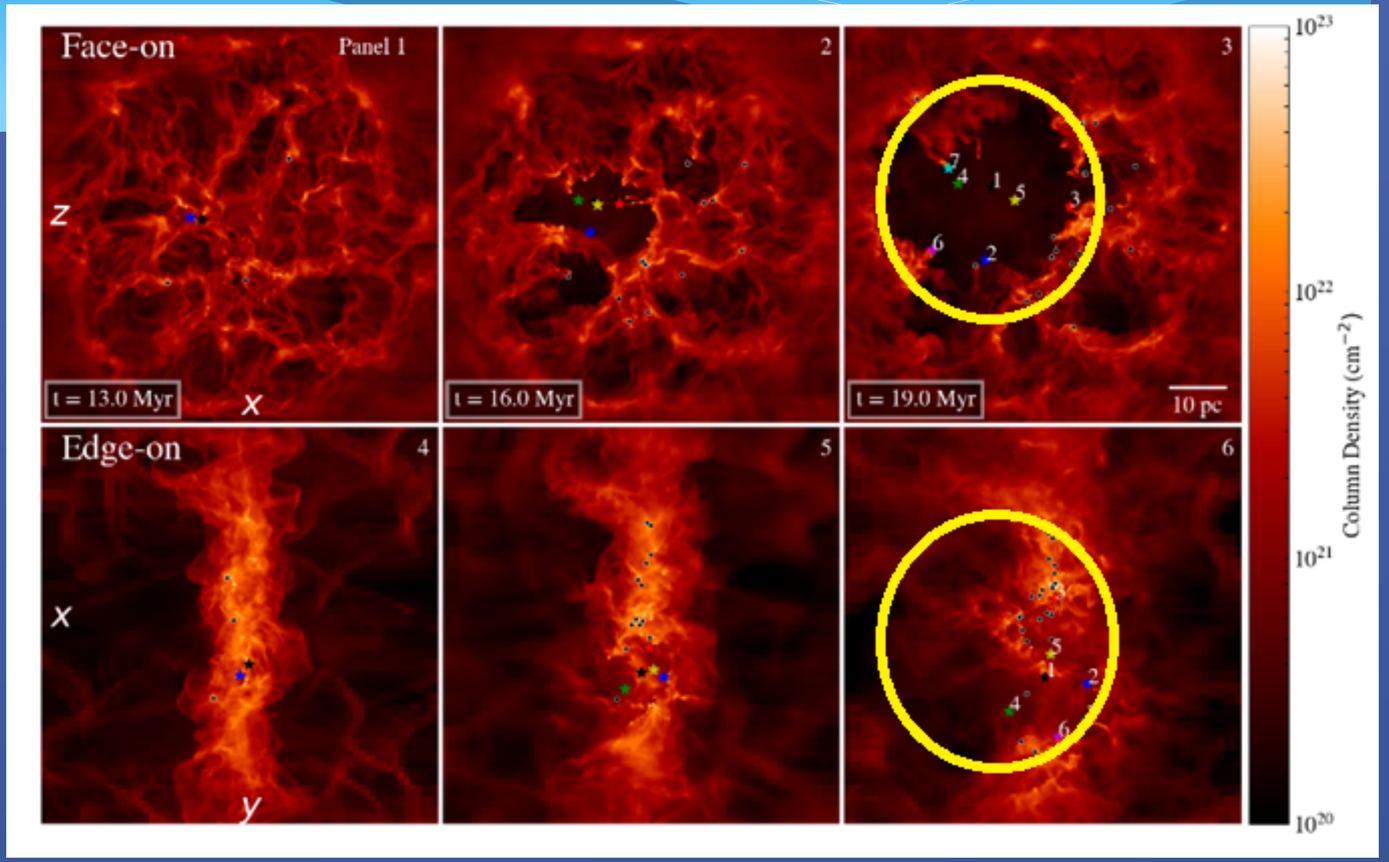

SNR SHOCK NOW INSIDE SWB

n_in =1e(-2)cm(-3)

n_swb_shell = 50 cm(-3) =4 x 12 cm(-3), n_ism =12 cm(-3)

arXiv:1907.04316v1

OUR MODELS OF GAMMA-RAY EMISSION

HADRONIC MECHANISM

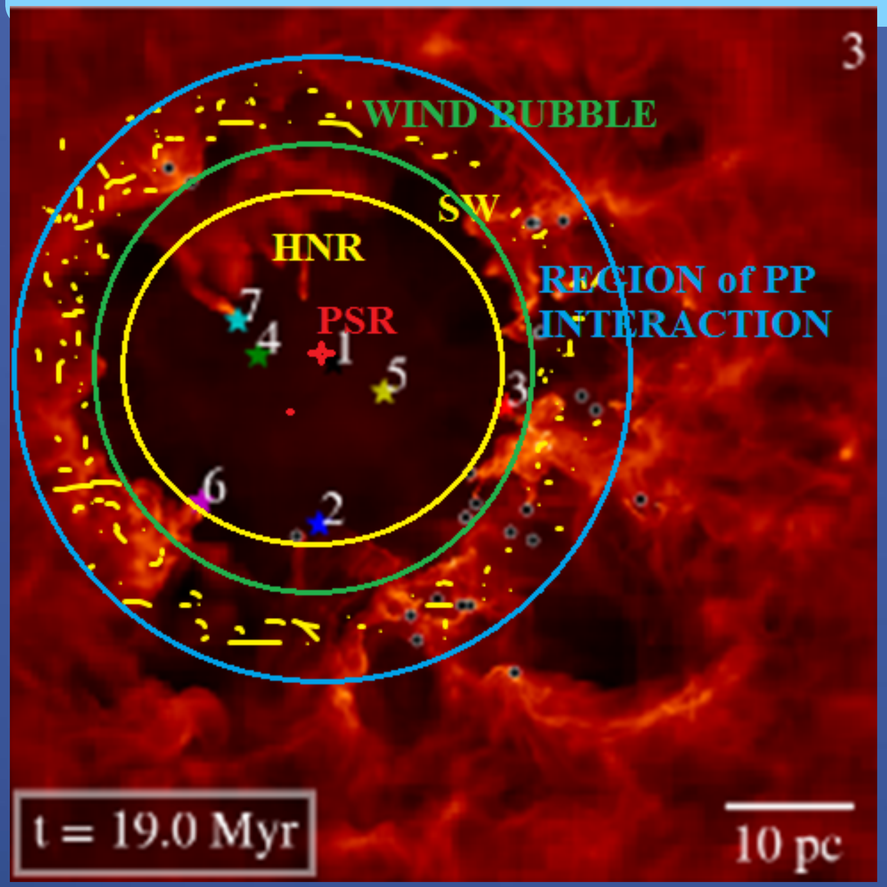

LEPTONIC MECHANISM

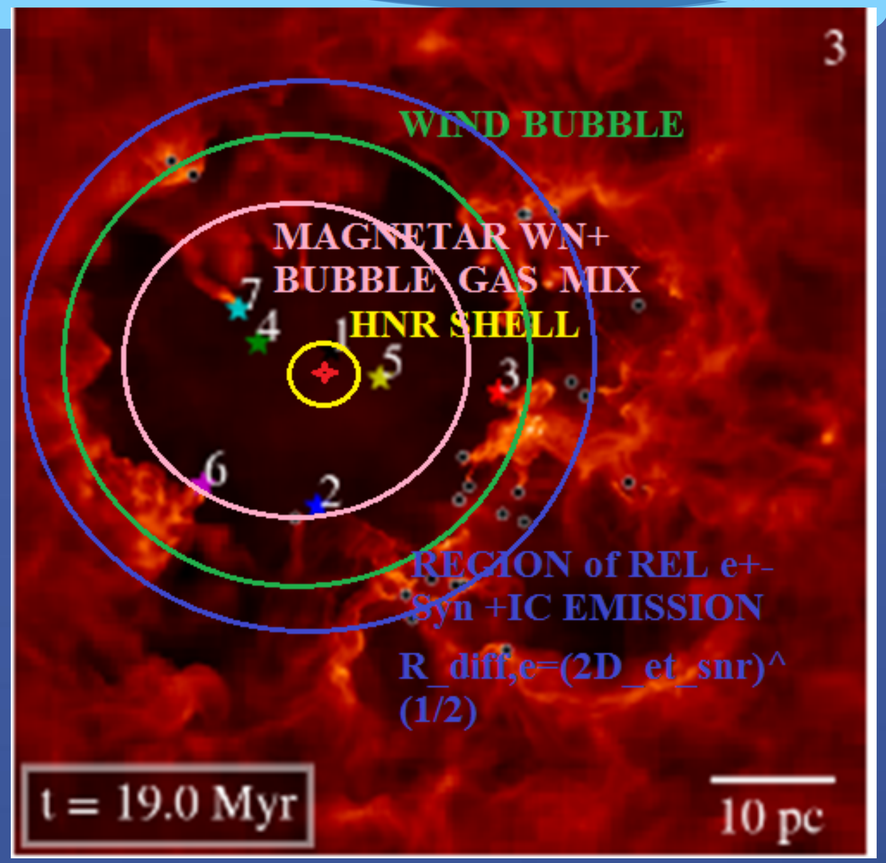

R_diff=(2D_pt_snr)^(1/2)≈20-40 pc

SED modelling in case of MWN model with 2 component ECPL lepton spectrum

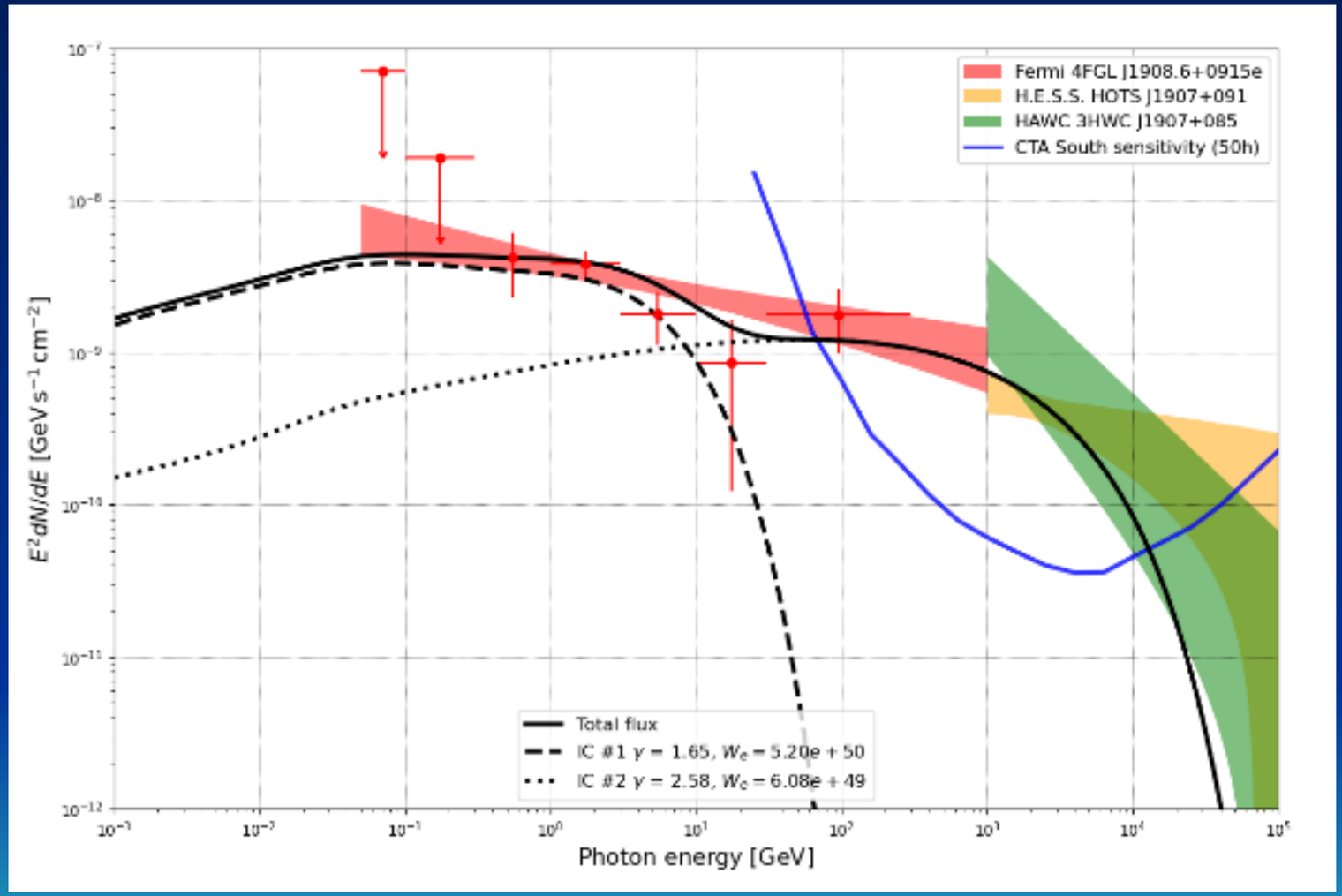

Best-fit spectrum corresponds to

$W_{e,1} = 5.2 \times 10^{50}$ **erg,** $W_{e,2} = 6.1 \times 10^{49}$ **erg**

Slide about leptonic mechanism